



Design and Realisation of a Synthetic Aperture Radar Transmitter

Nicolas Gréant

Final degree project submitted with a view to obtain
the degree of Master of Applied Sciences: EIT

Tutors:

Prof. Dr. ir. Yves Rolain (VUB)

Prof. Dr. ir. Paco López-Dekker (UPC)

Faculty of Engineering - Department ELEC (VUB)

Faculty of Engineering - Department TSC (UPC)

Academic Year 2008-2009

Cada hombre es el hijo de su propio trabajo
(Every man is the son of his own works)

-Miguel de Cervantes Saavedra-

Preface

If working on a university project represents hard labour but also satisfaction when the objectives are reached, then the successful accomplishment of a time-consuming master degree project feels like something to be really proud of. For the first time in your academic history, you created something autonomously, something of which can be spoken about, something which will be indelibly stamped in your memory. And I'm highly satisfied that I could do research on a topic which was truly one of my interest: very practical analog microwave design and layout with in the end a tangible outcome.

For me there was the additional challenge of working on this project with new people in a new environment, at 1357 km from what is called 'home'. This challenge also included difficulties like a new language, a generally slower long-distance communication and the tackling with an independent life in an inviting cultural metropolis.

But the successful realization wouldn't have been possible without the 'intensive care' of:

- Yves Rolain and Gerd Vandersteen, my tutors at VUB,
- Paco López-Dekker and Jordi Mallorquí, my tutors at UPC,
- Juan Carlos Merlano, my 'anytime' adviser,
- Ruben and Albert, the technicians,
- Katy, for the weekly tips & tricks,
- my parents, for their motivating calls,
- Sofie, for the support and love all the way to the finish.

Thank you all for bringing this project to what it had to become!

Summary

In this master degree project a Synthetic Aperture Radar (SAR) transmitter is designed and realized. This transmitter will be used in the Signal Theory and Communications lab of Universitat Politècnica de Catalunya as a test transmitter because the actual transmitters, which are two satellites from the European Space Agency, only provide a few seconds of testing every few weeks. This is not sufficient to continuously improve the sophisticated receiver subsystems.

It was mainly focussed on the design, layout and building of the analog microwave subsystems but also some programming skills were necessary to generate the required input signal.

By means of two synchronized direct digital synthesizers, two linearly frequency sweeping signals (chirps) at low-frequency band (base band) are generated and two mixers upconvert these signals to a high-frequency band around a carrier at 5.3 GHz. The carriers are provided by a quadrature hybrid, which splits the high-frequency sine wave from the local oscillator in an in-phase signal and a signal 90 degrees shifted in phase to the latter one (quadrature signal). Both outputs from the mixers are recombined by a power combiner, filtered and amplified by a low-noise amplifier and a power amplifier to obtain the required test signal.

The testing of the transmitter was a great success in which theory went hand in hand with practice. The realization of this project will be one of the required assets for further groundbreaking developments in the SAR research domain.

Contents

| | | |
|----------|--|-----------|
| 1 | Introduction | 2 |
| 1.1 | Assignment | 3 |
| 1.2 | Approach | 3 |
| 2 | Literature Study: Pulsed Radars | 4 |
| 2.1 | Introduction | 5 |
| 2.2 | Block Diagram | 6 |
| 2.3 | Resolution, Ambiguity and Blind Distance | 7 |
| 2.3.1 | Resolution | 7 |
| 2.3.2 | Ambiguity | 8 |
| 2.3.3 | Blind Distance | 9 |
| 2.4 | Radar Cross Section | 9 |
| 2.5 | Antennas and Propagation. Radar Equation | 10 |
| 2.6 | Angular Resolution. Uncertainty Volume | 11 |
| 2.7 | SNR in Radar. Radar Equation (2) | 12 |
| 2.8 | Probability of Detection. Probability of False Alarm | 13 |
| 2.9 | Pulse Integration | 15 |
| 2.9.1 | Coherent integration | 15 |
| 2.9.2 | Incoherent integration | 16 |
| 2.9.3 | Binary integration | 16 |
| 2.10 | Propagation and Loss in Radar Signals | 18 |
| 2.11 | Monostatic versus Bistatic Radar | 18 |
| 2.12 | Synthetic Aperture Radar | 19 |
| 3 | Overview of the Transmitter | 22 |
| 3.1 | Preliminary Study of the Transmitter | 23 |
| 3.1.1 | Satellite Signal Characteristics | 23 |
| 3.1.2 | SSB Modulation with an IQ Modulator | 23 |
| 3.1.3 | Block Diagram | 25 |
| 3.1.4 | Frequency Budget | 26 |
| 3.1.5 | Power Budget | 28 |
| 3.1.6 | Phase Noise | 28 |
| 3.1.7 | Substrate Characteristics | 29 |
| 3.2 | Simulation & Layout Tools | 31 |

| | | |
|----------|---|-----------|
| 4 | Base Band Subsystems | 33 |
| 4.1 | Direct Digital Synthesizer | 34 |
| 4.1.1 | Linear Sweep Mode | 37 |
| 4.1.2 | Automatic Synchronization of both DDS's | 37 |
| 4.1.3 | Frequency Sweep | 37 |
| 4.1.4 | Quadrature Phase Offset | 38 |
| 4.1.5 | Clear the Phase Accumulator | 38 |
| 4.1.6 | Measurements | 39 |
| 4.2 | Low-Pass Filter | 43 |
| 5 | High-Frequency Subsystems | 46 |
| 5.1 | Wilkinson Quadrature Hybrid | 47 |
| 5.2 | Mixer | 53 |
| 5.2.1 | Nonlinear Behaviour | 53 |
| 5.2.2 | ADS Mixer Model | 54 |
| 5.3 | Power Combiner | 57 |
| 5.4 | IQ Modulator | 63 |
| 5.5 | Band-Pass Filter | 68 |
| 5.6 | Low-Noise Amplifier and Power Amplifier | 74 |
| 6 | Conclusion | 76 |
| | Bibliography | 78 |

Chapter 1

Introduction

1.1 Assignment

At the department of Signal Theory and Communications (TSC), part of the Universitat Politècnica de Catalunya (UPC) in Barcelona (Spain), a team of engineers is currently working on a particular innovative radar system. They are developing a bistatic Synthetic Aperture Radar (SAR) system (more information in sections 2.1 and 2.12) that uses existing orbital SAR systems as transmitters of opportunity. The project has been going on for some time, and they have already produced some interesting results (Ref. [12]).

Relying on the satellite implies that they often need to wait a number of weeks for only a few seconds of testing. Thus, as the system is getting more sophisticated it has become more important to have their own test transmitter. Not having its own transmitter hinders the testing and, therefore, further development of all the other subsystems (receive RF front-end, data acquisition, synchronization hardware/software, etc.). Obviously, having a reliable transmit subsystem opens a range of experimental possibilities, since they then have all the necessary to implement a full radar.

How the design and realization of this Synthetic Aperture Radar transmitter is done, will be described in the following.

1.2 Approach

Before enlarging on the transmitter in detail, first some basic knowledge about the fundamental principles of pulsed radars and especially SAR is required. This is discussed in chapter 2.

A preliminary study will demonstrate that the realization of this SAR transmitter is practically achievable. Chapter 3 gives an overview by means of a block diagram together with a brief description of what the subsystems do and why they were chosen. Also, the choice of the tools which were used to simulate the subsystems and produce the layouts is discussed.

The specifications, simulation results and layouts of the base band (low-frequency) subsystems are handled in chapter 4. The measurements with oscilloscope, spectrum and network analyzer are shown and conclusions are taken.

In chapter 5 the same topics are discussed but now for the high-frequency subsystems.

Finally in chapter 6 an overall conclusion should make clear that this project was a success, both for the researcher as for the successful working of the transmitter.

Chapter 2

Literature Study: Pulsed Radars

2.1 Introduction

The term RADAR stands for Radio Detection And Ranging. A radar is a device that detects objects, which are called targets using an electromagnetic beam. The operation of a radar is shown in Figure 2.1. When the beam hits the target, a part of the beam is reflected. This reflection propagates back to the receiver, where it is detected. When one measures the time-of-flight of the beam, the range (1D) and/or the position (2D or 3D) of the object can be measured.

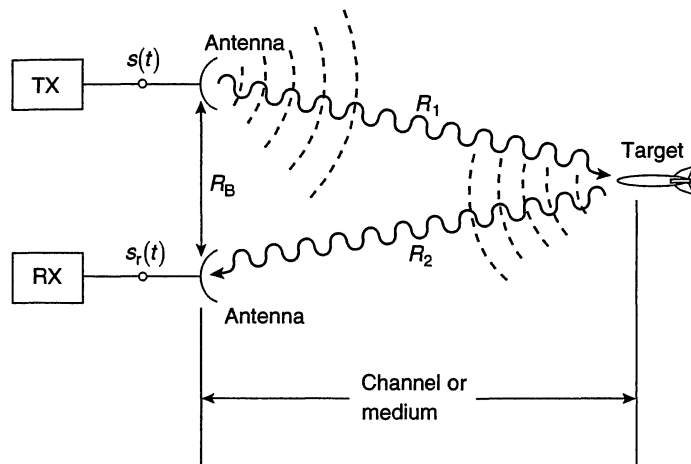


Figure 2.1: Basic principle of radar (Ref. [10])

The two most important types of radars are classified based on the type of beam that is used: pulsed radar and continuous-wave (CW) radar.

The latter is a radar system where an RF bundle (usually with constant amplitude) is continuously transmitted with or without frequency modulation, and the return frequencies are shifted away from the transmitted frequencies based on the Doppler effect. The main advantage of CW radars is that they are not as complex as pulsed radars. But pulsed radars are often preferred over CW radars because isolation between transmitter and receiver is necessary for long ranges. The receiver of a pulsed radar can be inhibited during transmission which is not possible in CW radar systems as these are transmitting continuously.

In the following we will only discuss the pulsed radar as this is the most widely used setup and in section 2.12 will be explained that the transmitter of this project is based on a pulsed radar system too. Pulsed radar is a radar system where periodically repeating pulses of RF energy are transmitted (see Figure 2.2). The time period between two transmitted pulses or the Pulse Repetition Interval (PRI) is defined as T , the duration of a transmitted pulse is defined as T_0 and the duration of a received pulse in the case of a radar system without

pulse compression¹, measured at half amplitude, is defined as τ_0 . The Pulse Repetition Frequency (PRF) is equal to $\frac{1}{T}$.

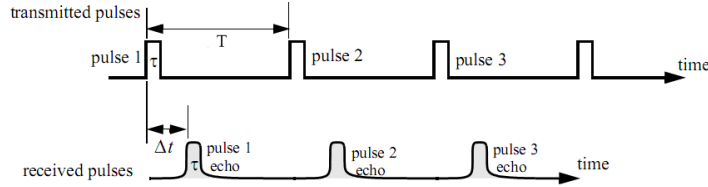


Figure 2.2: Time plan of transmitted and received pulses (Ref. [6])

The range R is obtained by a measurement of the time-of-flight Δt , i.e. the time delay between the transmitted and the received pulses. As an electromagnetic beam is propagating at the speed of light $c = 3 \times 10^8 m/s$, the following formula can be used:

$$\text{time - of - flight } \Delta t = \frac{\text{distance to target and back } (2R)}{\text{speed of light } (c)} \quad (2.1)$$

or $\Delta t = \frac{2R}{c}$

In this way we derive a formula for the range R :

$$R = \frac{\Delta t \times c}{2} \quad (2.2)$$

2.2 Block Diagram

With the aid of the block diagram shown in Figure 2.3 the operation of a simple pulsed radar system can be explained.

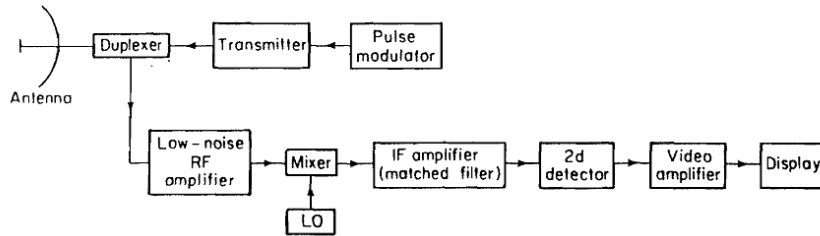


Figure 2.3: Block diagram of a pulsed radar system (Ref. [14])

¹Pulse compression is a technique to increase the Signal-to-Noise Ratio (SNR) at the receiver by transmitting a long modulated pulse that has a bandwidth B corresponding to a short pulse to as well increase the range resolution (see section 2.3.1). In this case τ_0 would be equal to $\frac{\text{duration of the long pulse}}{\text{duration of the corresponding short pulse}} \times \frac{1}{B}$

The transmitter can be an oscillator: the modulator then turns it off and on to obtain pulsed signals. These pulses propagate via a transmission line to the antenna, where they are radiated. In general the same antenna is also a receiver for incident RF bundles.

The duplexer permits the receiver and transmitter to share a common antenna, while isolating both because the receiver has to be protected from high power of the transmitter.

Using a low-noise amplifier (LNA), the noise of all the subsequent stages is dominated by the gain of the LNA, while the noise of the LNA itself is injected directly into the received signal. That is why this so-called low-noise amplifier has to boost the signal with a minimal addition of noise.

The mixer and local oscillator (LO) downconvert the RF signal to an intermediate frequency (IF).

The IF amplifier was originally designed as a matched filter², i.e. its frequency-response function $H(f)$ should maximize the peak-signal-to-mean-noise-power ratio at the output. Nowadays this is done in the digital processing subsystem.

Finally, the pulses are demodulated by the second detector and amplified by the video amplifier to a level where they can be properly displayed.

2.3 Resolution, Ambiguity and Blind Distance

2.3.1 Resolution

The resolution is defined as the minimum range separation ΔR at which two different targets at the same azimuth and elevation angles can be distinguished. (Ref. [7])

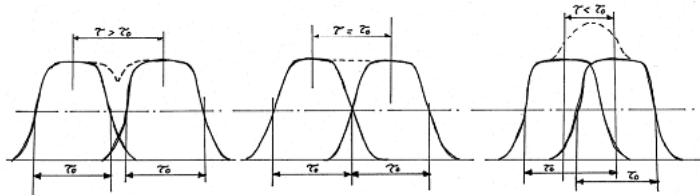


Figure 2.4: Time separation between two pulses

If we define τ as the time between both maximum amplitudes of the two pulses, we can consider three theoretical situations (see Figure 2.4):

- $\tau > \tau_0$
- $\tau = \tau_0$
- $\tau < \tau_0$

²A more detailed discussion of the matched filter is not within the scope of this project.

In the first situation the overlap of the two pulses still results in two peaks and we can still distinguish the two targets. In the second situation the overlap of the two pulses results in one pulse with duration $2\tau_0$ and we cannot distinguish the two targets anymore. In the third situation the overlap results in one peak and the two targets are not distinguishable anymore neither. These situations are of course purely theoretical because, in practice for the case of $\tau = \tau_0$, the overlap of the two pulses will not be perfectly flat and still several small peaks could induce one to distinguish several targets.

As $\tau = \tau_0$ is the minimal time separation between two targets, the minimal radial separation is accordingly:

$$\Delta R = \frac{\tau_0 \times c}{2} \quad (2.3)$$

However, this formula is only valid for the specific case of square pulses in radars without pulse compression where $\tau_0 = \frac{1}{B}$ with bandwidth B of the pulse (or the matched filter) . In general $\tau_0 > \frac{1}{B}$ and the resolution depends on the bandwidth as:

$$\Delta R = \frac{c}{2B} \quad (2.4)$$

2.3.2 Ambiguity

The maximum non-ambiguous distance R_{amb} is defined as the maximum distance between a radar and a target at which a received pulse can be unconditionally considered as the response to a given transmitted pulse.

It can be easily shown that this distance is:

$$R_{amb} = \frac{T \times c}{2} \quad (2.5)$$

because if a received pulse would not fall in the same pulse repetition interval (PRI) as the transmitted pulse, i.e. $\Delta t > T$, the received pulse could be ambiguously matched to a response of the next transmitted pulse in the next PRI of a target more close by (see Figure 2.5). Therefore the limit is $\Delta t = T$ and formula 2.5 follows.

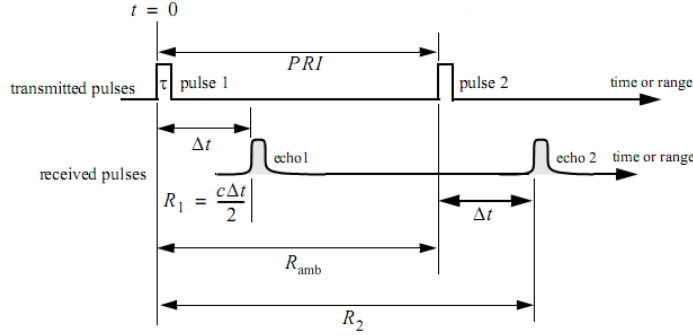


Figure 2.5: Ambiguity because $\Delta t > T$ (Ref. [6])

The maximum non-ambiguous distance can be increased by using several pulse repetition frequencies (PRF), this technique is called “staggering”.

2.3.3 Blind Distance

As said in section 2.1, the receiver is inhibited during transmission with duration of T_0 and as a result responses from targets located nearby won't be measured.

The so-called blind distance is the distance from where responses can be measured again and it is given by:

$$R_{blind} = \frac{T_0 \times c}{2} \quad (2.6)$$

2.4 Radar Cross Section

The Radar Cross Section (RCS) is a measure of the reflective strength of a radar target and is defined as (Ref. [7]):

$$\sigma = \frac{(4\pi R^2) \times (\text{power density re - radiated towards the radar } P_r)}{(\text{incident power density at the target } P_i)} \quad (2.7)$$

This can be written as:

$$\sigma = \lim_{R \rightarrow \infty} 4\pi R^2 \frac{|E_r|^2}{|E_i|^2} \quad (2.8)$$

where E_r and E_i are the re-radiated (or scattered) and incident electric field intensities respectively.

The unit of RCS is $(\text{meter})^2$ and can be given in logarithmic scale:

$$\sigma (\text{dBsm}) = 10 \times \log_{10} \left(\frac{\sigma (\text{m}^2)}{1 \text{ m}^2} \right) \quad (2.9)$$

The power re-radiated towards the radar is the amount of power that a theoretical isotropic antenna would emit to produce the peak power density observed in the direction of maximum antenna gain. This is called the Equivalent Isotropically Radiated Power (EIRP).

In this way we can also write:

$$\sigma = \lim_{R \rightarrow \infty} \frac{EIRP}{P_i} \quad (2.10)$$

2.5 Antennas and Propagation. Radar Equation

To determine the power received at the radar, the radar equation is used. To derive this equation, the power budget of the signal sent at the transmitter towards the target and back to the receiver is determined:

1. The radiated power for an isotropic transmitter antenna is written as P_r . In the most common case, a directive antenna is used and this gives a radiated power of $P_r \times D$ with D : the directivity of the antenna. This power is the previously defined Equivalent Isotropically Radiated Power (*EIRP*), see section 2.4.
2. If the range is written as R , the incident power density at the target then is:

$$\text{incident power density at the target} = \frac{P_r \times D}{4\pi R^2} \quad (2.11)$$

3. With the previous definition of the Radar Cross Section (RCS) in section 2.4, $\sigma = \frac{EIRP}{\text{incident power density}}$, the power re-radiated towards the radar (in this case also *EIRP*) then is:

$$\text{power reradiated towards the radar} = \frac{P_r \times D}{4\pi R^2} \times \sigma \quad (2.12)$$

4. The power density received at the radar then would be:

$$\text{power density received at the radar} = \frac{P_r \times D}{4\pi R^2} \times \sigma \times \frac{1}{4\pi R^2} \quad (2.13)$$

5. The Antenna Effective Area (A_{eff}) is defined as the equivalent area from which an antenna directed towards the source of the received signal absorbs the incident energy. The power received at the radar is accordingly:

$$\text{power received at the radar} = \frac{P_r \times D}{4\pi R^2} \times \sigma \times \frac{1}{4\pi R^2} \times A_{eff} \quad (2.14)$$

And as a consequence of electromagnetic reciprocity

$$A_{eff} = \frac{\lambda^2}{4\pi} \times D \quad (2.15)$$

can be derived³.

6. If we also consider the loss of the lines, propagation, polarization, ... in a term L , the complete radar equation then becomes:

$$\text{Power receiver at radar} = \frac{P_r \times D^2 \times \sigma \times \lambda^2}{(4\pi)^3 \times R^4 \times L} \quad (2.16)$$

2.6 Angular Resolution. Uncertainty Volume

Tangential resolution can be defined as the ability to discern two separate point targets. This feature can be achieved by using a directive antenna beam.

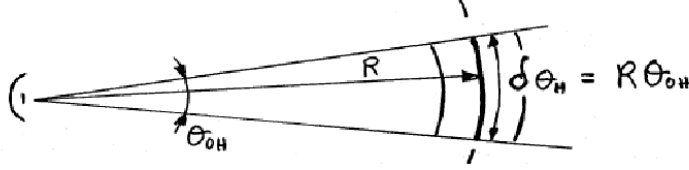


Figure 2.6: Azimuth tangential resolution (Ref. [2])

The azimuth tangential resolution $\delta\theta_H$ is related to the beamwidth θ_{OH} and the target distance R :

$$\delta\theta_H = R \times \theta_{OH} \quad (2.17)$$

(see Figure 2.6). In an analogous way the elevation tangential resolution can be found:

$$\delta\theta_V = R \times \theta_{OV} \quad (2.18)$$

The uncertainty volume (V_u) is the volume of a resolution cell, limited by the size of the range resolution and the two tangential resolutions (see Figure 2.7). It follows that:

$$V_u = \delta\theta_H \times \delta\theta_V \times \Delta R = \theta_{OH} \times \theta_{OV} \times R^2 \times \Delta R = \Omega \times R^2 \times \Delta R \quad (2.19)$$

with $\Omega = \theta_{OH} \times \theta_{OV}$

³The derivation of A_{eff} is not within the scope of this project.

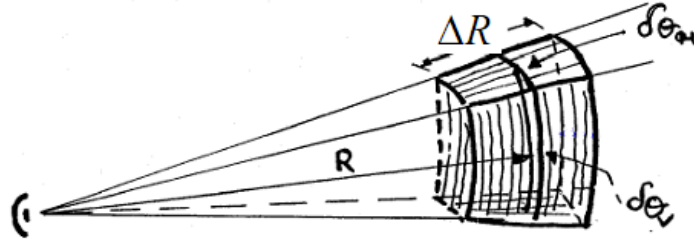


Figure 2.7: Resolution cell (Ref. [2])

Within these cell multiple targets cannot be distinguished except by their Doppler frequencies, i.e. their radial velocity with respect to the radar.

2.7 SNR in Radar. Radar Equation (2)

In this part the Signal-to-Noise Ratio is derived and accordingly a second, equivalent radar equation is set up.

The noise power P_n can be determined as:

$$P_n = k \times T_a \times B \quad (2.20)$$

with

$k = 1,38 \times 10^{-23} \frac{J}{K}$ (Boltzmann's constant)

T_a = antenna noise temperature

B = bandwidth of the receiver

The noise power in practical receivers is often greater than can be accounted for by thermal noise alone. The total noise at the output of the receiver may be considered to be equal to the thermal-noise power obtained from an "ideal" receiver multiplied by a factor called noise figure.

In an amplifier stage noise figure F is used:

$$F = 1 + T_e/T_0 \quad (2.21)$$

with T_e = equivalent noise temperature

T_0 = standard noise temperature

The Signal-to-Noise Ratio (SNR) then becomes:

$$SNR = \frac{S}{N} = \frac{P_T G^2 \sigma \lambda^2}{(4\pi)^3 R^4 k T_0 F B L} \quad (2.22)$$

2.8 Probability of Detection. Probability of False Alarm

The signal gathered by the antenna is forwarded to a detector where a decision is taken regarding detection of a target. The probability of detection (P_d) and the probability of false alarm (P_{fa}) quantify the quality of this decision.

Three important situations can occur during the decision-making of the detector, depending on the threshold level V_t :

- Loss: the signal does not rise above the threshold and is not detected ($V < V_t$).
- False alarm: noise alone rises above the threshold and is taken for a real signal ($V > V_t$), see Figure 2.8 for an illustration.
- Detection: the signal which rises above the threshold is detected correctly ($V > V_t$).

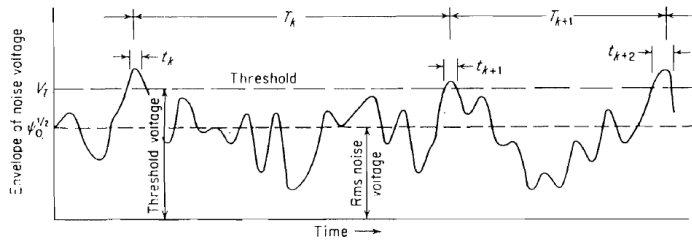


Figure 2.8: Envelope of receiver output illustrating false alarms due to noise (Ref. [14])

Now consider the probability-density function (pdf) for noise alone and for signal-plus-noise (Figure 2.9). The first depends on the power of noise and unwanted echoes (called clutter) and its statistics. The latter depends on the power of the target RCS statistics.

P_d can be calculated by integrating the subtraction of the signal-plus-noise pdf with the noise alone pdf between V_t and ∞ (single-striped area).

P_f can be calculated by integrating the noise alone pdf between V_t and ∞ (double-striped area).

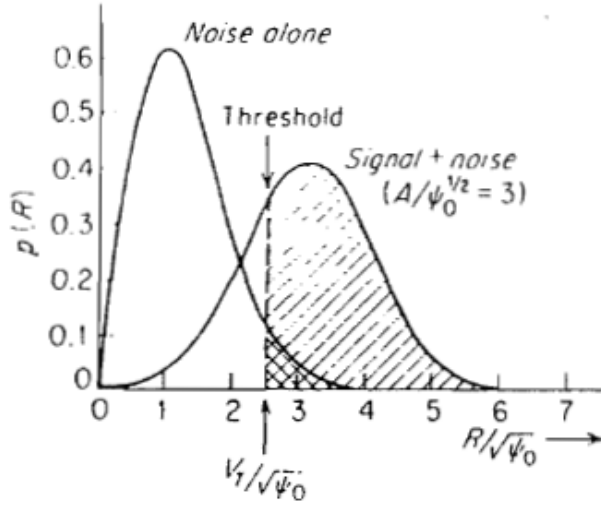


Figure 2.9: Probability-density function for noise alone and for signal-plus-noise (Ref. [14])

If the targets can be modeled by many small reflecting objects with more or less an equal RCS, the following formula can be used, relating P_d , P_{fa} and SNR :

$$P_d = P_{fa}^{\frac{1}{1+SNR}} \quad (2.23)$$

The average number of cells explored between two false alarms is:

$$N \approx \frac{1}{P_{fa}} \quad (2.24)$$

And as the time spent exploring a cell is, at least $1/B$, thus:

$$T_{fa} \geq \frac{1}{B \times P_{fa}} \quad (2.25)$$

The probability of detection can be increased by taking into account consecutive antenna scans (K):

P_d : probability of detection for a single scan

$1-P_d$: probability of loss for a single scan

$(1 - P_d)^K$: probability of loss for K scans

$1 - (1 - P_d)^K$: probability of detection for K scans

2.9 Pulse Integration

An integrator is a device that combines several pulses received in a scan to improve the probability of detection. Three types are considered:

- coherent integrators combine pulses before the detector.
- incoherent integrators combine pulses after the detector and before the comparator.
- binary integrators combine the outputs of the comparator for a given resolution cell.

In a 2D radar the maximum number of pulses that can be integrated in a scan is:

$$n \leq (\text{observation time } t_{obs}) \times (\text{pulse repetition frequency } PRF) \quad (2.26)$$

The observation time t_{obs} is the time that the main beam of the antenna illuminates the target.

If the antenna is rotating with an angular velocity ω and its horizontal beamwidth is θ_{OH} then t_{obs} is:

$$t_{obs} = \frac{\theta_{OH}}{\omega} \quad (2.27)$$

And accordingly, n becomes:

$$n \leq \frac{\theta_{OH}}{\omega} \times PRF \quad (2.28)$$

For a 3D radar with mechanical rotation in azimuth and uniform electronic steering in elevation, the observation time and number of pulses are reduced in proportion to the ratio of vertical beamwidth (θ_{OV}) and vertical exploration range (θ_V):

$$n \leq \frac{\theta_{OH}}{\omega} \times PRF \times \frac{\theta_{OV}}{\theta_V} \quad (2.29)$$

2.9.1 Coherent integration

Received pulses have to be added in phase to obtain an effective integration. Also the target should maintain a constant (or slow-varying) RCS during observation time. Ideally n signal pulses are added in phase together with n uncorrelated noise samples.

Considering that the output signal power (S_n) will be n^2 times that of a single pulse (S_1), and the output noise power (N_n) will be only n times that of the output noise power without integration (N_1):

$$\left(\frac{S_n}{N_n}\right) = \frac{n^2}{n} \times \frac{S_1}{N_1} = n \times \frac{S_1}{N_1} \quad (2.30)$$

In practice, the received pulses are not perfectly added in phase and therefore an “integration efficiency” E_i is taken into account.

The radar equation with integration then becomes:

$$SNR = \frac{S}{N} = \frac{P_T G^2 \sigma \lambda^2 n E_i}{(4\pi)^3 R^4 k T_0 F B L} \quad (2.31)$$

2.9.2 Incoherent integration

In radar systems with incoherent integration the pulses do not have to be added in phase, so it is technologically simpler to implement such a receiver. Therefore more pulses can be integrated than with coherent integration but, for a given number of pulses, the efficiency is lower.

The improvement in SNR can be derived through the integration-improvement factor $I(n)$, as shown in Figure 2.10.

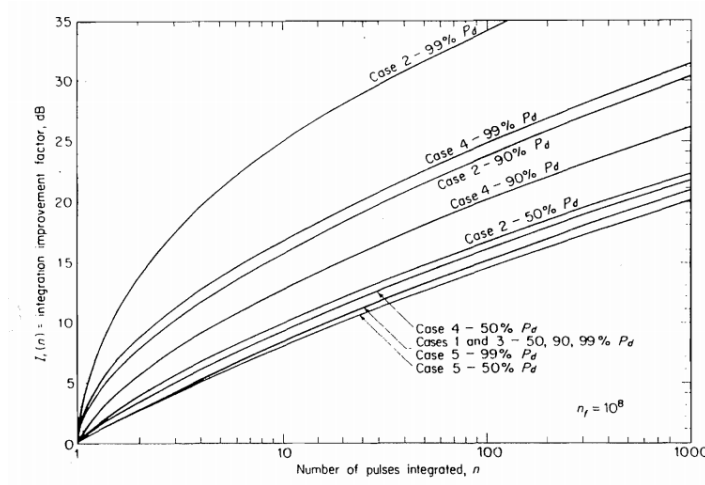


Figure 2.10: Integration-improvement factor as a function of the number of pulses integrated (Ref. [14])

2.9.3 Binary integration

By using several pulse repetition frequencies (PRF), the ambiguous distance can be increased. Only the pulse echo that matches for all PRF's in the time plan, shown in Figure 2.11, will be considered.

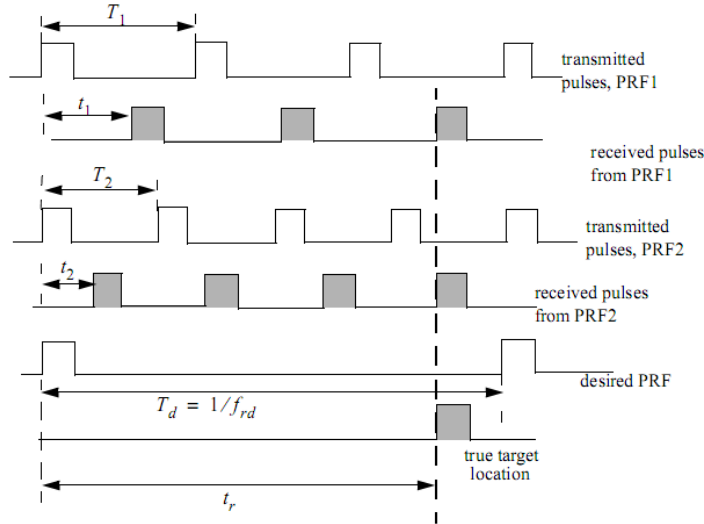


Figure 2.11: Resolving range ambiguity by only considering the matching pulses (Ref. [6])

The process of decision making consists of two consecutive steps: first one at the level of each PRF and a second one at the level of all PRF's in a given scan (see Figure 2.12). Denote P_{d1} as the probability of detection for a single PRF and P_{d2} for all combined PRF's, then P_{d2} can be written as:

$$P_{d2} = \sum_{i=M}^N \binom{N}{i} (P_{d1})^i (1 - P_{d1})^{N-i} \quad (2.32)$$

And analog for the probability of false alarm:

$$P_{fa2} = \sum_{i=M}^N \binom{N}{i} (P_{fa1})^i (1 - P_{fa1})^{N-i} \quad (2.33)$$

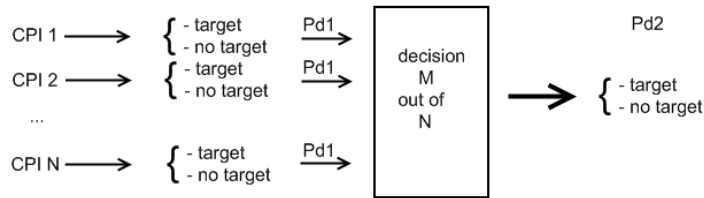


Figure 2.12: Binary integration, multiple decision stages

2.10 Propagation and Loss in Radar Signals

In the frequency for which Rayleigh scattering applies (particles small in size compared with the wavelength) there is attenuation of the radar signals due to absorption. This is relevant for rain, like shown in Figure 2.13, with a dependency of wavelength and rainfall rate.

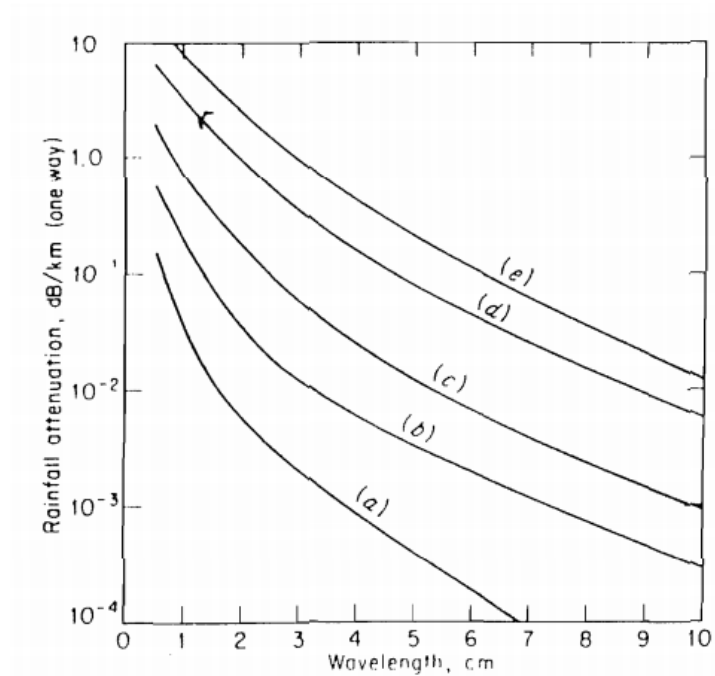


Figure 2.13: One-way attenuation (dB/km) in rain at a temperature of 18°C. (a) Drizzle - 0.25 mm/h; (b) light rain - 1 mm/h; (c) moderate rain - 4 mm/h; (d) heavy rain - 16 mm/h; (e) excessive rain - 40 mm/h (Ref. [14])

2.11 Monostatic versus Bistatic Radar

In general, transmitting and receiving stations can exist at the same location (monostatic radar) or can have different locations (bistatic radar). The latter system has some advantages:

- several bistatic receivers can be used, each of them pointing at the same location and combining measurements
- there is no need for isolation between the transmitter and the receiver as they are not on the same location

- if the transmitter is provided (e.g. satellite), a potentially simple and cheap receiver can be build
- as the receiver's location is potentially unknown, electronic countermeasures (e.g. jamming) are more difficult and covert operation is possible

But bistatic radar also has some disadvantages compared to monostatic radar:

- the system is more complex
- the transmitter is not always easily controllable as it is on a different location (e.g. in space)
- the receiver needs to be synchronized to the transmitter

2.12 Synthetic Aperture Radar

Synthetic Aperture Radar (SAR) is a radar system which synthesizes a large antenna to obtain a high azimuth resolution. It measures the range in the same way as the conventional pulsed radar does (see section 2.1) and measures azimuth perpendicular to the range. As the microwave frequency of the transmitted signals is low compared to optical systems, antenna lengths of several hundreds of meters would be needed to obtain the same resolution.

But if an aircraft could collect and store data, and recombine the stored data after flying this distance as if it came from a physically long antenna, a large antenna is simulated. This distance is known as the synthetic aperture and the larger the aperture is, the sharper the beam and therefore the higher the azimuth resolution. It is similar to a phased array⁴ but SAR uses only one antenna in time-multiplex (see Figure 2.14).

⁴Phased array: large number of parallel antenna elements in which the relative phases of the feeding element signals are varied in such a way that the directivity is sincerely improved.

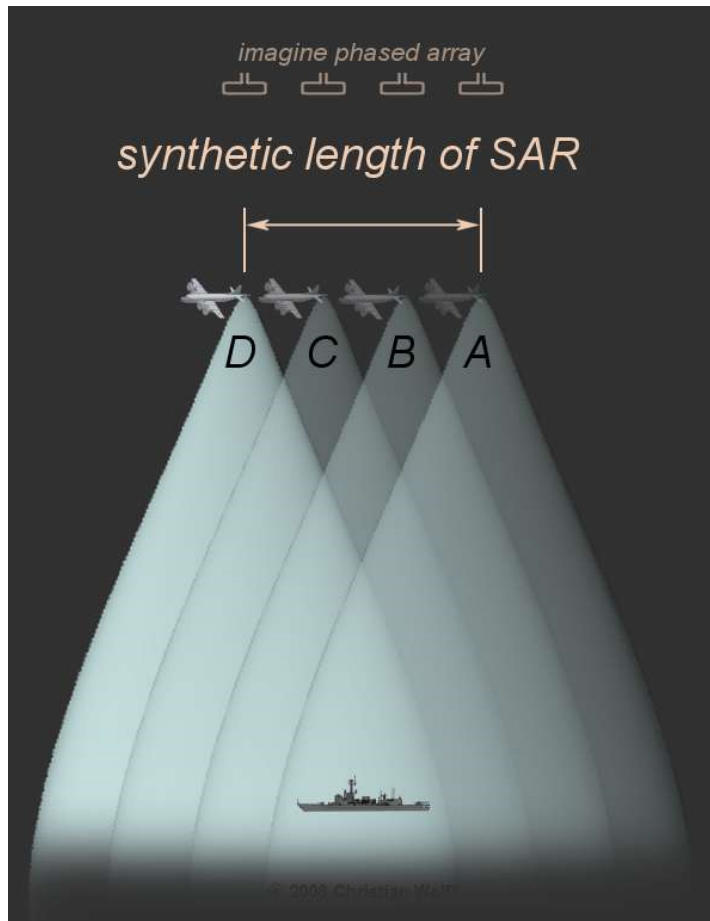


Figure 2.14: Principle of synthetic aperture radar, similar to a phased array

If the target is ahead of the plane, it produces a positive Doppler frequency⁵, if it is behind it produces a negative Doppler frequency. While the plane flies along the synthetic aperture, these Doppler frequencies can be measured and the azimuth position can be determined.

A SAR system therefore needs:

- a stable, coherent transmitter
- an efficient onboard data processor
- exact knowledge of the flight path and velocity of the plane

⁵The Doppler effect describes the change in frequency of a wave for an observer moving relative to the source of the waves. The change in frequency or Doppler frequency is positive when observer and source are moving towards each other and negative if they are moving away.

This radar system has some important advantages:

- it offers broad-area remote sensing imaging of the illuminated area
- high azimuth resolution (compared to other radars)
- functions even during inclement weather, and by day as well as at night

SAR is used for a list of applications: it can gather terrain structural information, detect oil spill boundaries on water, analyze the sea state and collect targeting information for military operations. The transmitters can also be on-board of a satellite of course. The synthetic aperture radar transmitters from the ERS-2 and ENVISAT satellites for example were launched in 1995 and 2002 respectively for Earth observation.

Chapter 3

Overview of the Transmitter

3.1 Preliminary Study of the Transmitter

3.1.1 Satellite Signal Characteristics

The orbital SAR systems from both satellites ERS-2 and ENVISAT from the European Space Agency (ESA) are currently used as transmitters of opportunity. The receiver RF front-end is designed to be able to process data in a bistatic set-up but also when pointing the receiver antenna directly to the transmitter. This involves that the test transmitter which is realized in this project should at least meet the receiver requirements such as the Signal-to-Noise Ratio (SNR) and be able to transmit the ERS-2 satellite signal (at the centre frequency of 5.300 GHz) and the ENVISAT satellite signal (at 5.331 GHz).

The SNR at the output of the receiver's front end is given by Friis' power transmission equation, when the receiving antenna is directly pointed towards the transmitter,

$$SNR = \frac{P_t \times G_t \times G_r \times \lambda_0^2}{(4\pi R_t)^2 \times k \times [T_{ant} + (F - 1)T_{sys}] B}, \quad (3.1)$$

with

$k = 1,38 \times 10^{-23} \frac{J}{K}$ known as the Boltzmann's constant,

T_{sys} as the system temperature,

T_a as the antenna noise temperature, significantly lower than T_{sys} because it is pointing almost at zenith: $T_a \ll T_{sys}$,

B as the signal bandwidth.

For ENVISAT the following (approximate) values can be used:

$B = 16 \text{ MHz}$, $P_t = 1500 \text{ W}$, $G_t = 45 \text{ dB}$, $\lambda_0 = \frac{c}{f} = \frac{3 \times 10^8 \text{ m/s}}{5.331 \times 10^9 \text{ Hz}} = 5,63 \text{ cm}$ and $R_t \approx 790 \text{ km}$

and assuming a noise figure F of 3 dB and a receive-antenna gain G_r of 18 dB, the minimum required SNR would be $\pm 61 \text{ dB}$.

We can assume that for this minimum required SNR , the maximum allowed phase noise of the test transmitter can be compared to the one which was studied in Ref. [13] in the typical case of using an ultra-stable oscillator (USO) at transmission level. The algorithm described in that article expects a phase error of roughly 0.1 radians.

3.1.2 SSB Modulation with an IQ Modulator

Suppose one provides two sinusoidal signals at the same frequency $f_{if} = \frac{\omega_{IF}}{2\pi}$ but shifted 90 degrees in phase from each other. Let's take one signal x_{i1} equal to a sine wave with a phase ϕ_1 , called the in-phase signal, and write it as:

$$x_{i1} = \sin(\omega_{IF}t + \phi_1) \quad (3.2)$$

Now let's take the other signal x_{q1} , 90 degrees shifted in phase to x_{i1} , called the quadrature signal, and write it as:

$$x_{q1} = \sin(90^\circ + \omega_{IF}t + \phi_1) = \cos(\omega_{IF}t + \phi_1) \quad (3.3)$$

Assume that x_{i1} and x_{i2} are connected to the intermediary frequency (IF) port of two similar upconverter mixers M1 and M2. If a local oscillator (LO) drives the LO-port of mixer M1 with a sine wave at frequency $f_{LO} = \frac{\omega_{LO}}{2\pi}$ and a phase ϕ_2 , and mixer M2 with a sine wave 90 degrees shifted in phase compared to ϕ_2 , then the resulting signals at the output RF-port of mixers M1 and M2 would be respectively:

$$x_{i2} = \sin(\omega_{LO}t + \phi_2) \times \sin(\omega_{IF}t + \phi_1) \quad (3.4)$$

$$x_{q2} = \sin(90^\circ + \omega_{LO}t + \phi_2) \times \cos(\omega_{IF}t + \phi_1) = \cos(\omega_{LO}t + \phi_2) \times \cos(\omega_{IF}t + \phi_1) \quad (3.5)$$

With the trigonometric identities this can also be written as:

$$x_{i2} = \frac{1}{2} \times (\cos[(\omega_{LO} - \omega_{IF})t + (\phi_2 - \phi_1)] - \cos[(\omega_{LO} + \omega_{IF})t + (\phi_2 + \phi_1)]) \quad (3.6)$$

$$x_{q2} = \frac{1}{2} \times (\cos[(\omega_{LO} - \omega_{IF})t + (\phi_2 - \phi_1)] + \cos[(\omega_{LO} + \omega_{IF})t + (\phi_2 + \phi_1)]) \quad (3.7)$$

The bandwidth BW of each individual signal would obviously be:

$$BW_I = BW_Q = \frac{1}{2\pi} [(\omega_{LO} + \omega_{IF}) - (\omega_{LO} - \omega_{IF})] = 2 \times f_{IF} \quad (3.8)$$

This gives a double side band (DSB), one left from f_{LO} and one right from f_{LO} on the frequency axis.

When those two signals would be combined, the resulting signal x_3 would become:

$$x_3 = x_{i2} + x_{q2} = \cos[(\omega_{LO} - \omega_{IF})t + (\phi_2 - \phi_1)] \quad (3.9)$$

As only one single side band (SSB) next to f_{LO} remains –in this case the lower side band– the bandwidth BW now is halved to:

$$BW_{IQ} = f_{IF} \quad (3.10)$$

To only obtain the upper side band, it is sufficient to invert signal x_{i2} as then x_3 would become:

$$x_3 = (-x_{i2}) + x_{q2} = \cos[(\omega_{LO} + \omega_{IF})t + (\phi_2 + \phi_1)] \quad (3.11)$$

3.1.3 Block Diagram

With the aid of the block diagram shown in Figure 3.1 the operation of the Synthetic Aperture Radar (SAR) transmitter can be explained. A profound discussion about the choice and properties of all blocks can be found in chapters 4 and 5.

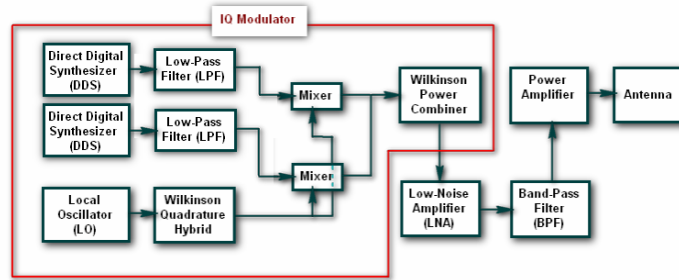


Figure 3.1: Block diagram of the SAR transmitter

To transmit radar pulses in a similar way as the ERS-2 and ENVISAT satellites, a data signal which is -in this case linearly- increasing in frequency from DC (0 Hz) to 8 MHz and decreasing again to DC, also known as chirp signal, should be generated. This can be done by a direct digital synthesizer (DDS).

The DDS is less sensible to phase errors in base band than for radio frequency (RF) as was described by Leeson (Ref. [8]). Therefore a mixer is used to upconvert the base band chirp to an RF frequency band (like the ESA satellites).

But a bad side-effect is that phase errors accumulate from chirp to chirp for such a set-up.

Another set-up would be the one of an IQ modulator: one DDS is used to generate an in-phase chirp signal and an other DDS for a quadrature chirp signal, i.e. 90 degrees shifted with respect to the in-phase signal. At the output of the both DDS's a low-pass filter removes the unwanted frequency component from the internal system clock. Then the quadrature and in-phase signals are applied on the Intermediary Frequency (IF) port of two upconverter mixers M1 and M2 respectively. A Wilkinson quadrature hybrid is used to symmetrically split the local oscillator signal in an in-phase and a quadrature signal, applied to the LO-port of mixers M1 and M2 respectively. Finally, both RF outputs of those mixers are recombined by a Wilkinson power combiner.

With this set-up, the phase for each repetition pulse period is much better controlled and the transmitter can send coherent pulses. This is very important for SAR systems.

A band-pass filter has the task to remove harmonic frequency components from the local oscillator (at $2 \times 5.3 \text{ GHz}$ and higher multiples of 5.3 GHz) and unwanted intermodulation products of the mixer (more details in section 5.5).

As will be explained in section 3.1.5, the signal power at the output of the power combiner is not high enough to acquire the transmitted signal at the receiver with a sufficient Signal-to-Noise Ratio (SNR). The amplification of one power amplifier would not meet this requirement but adding a second one would not be necessary either. A low-noise amplifier (LNA) which is available in the TSC lab and which amplifies more than half of what the power amplifier does is adequate. The LNA, which has a better noise behaviour than the power amplifier; is put before the latter one as per Friis' formula, the overall noise figure of a circuit is dominated by the first few stages¹.

3.1.4 Frequency Budget

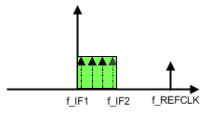
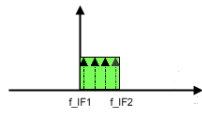
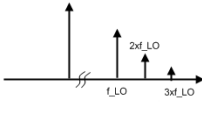
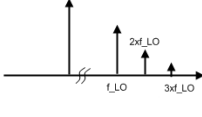
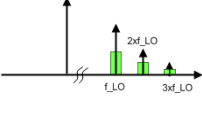
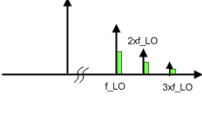
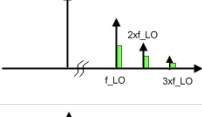
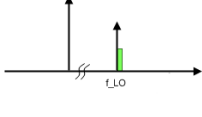
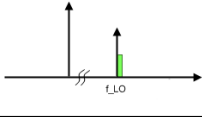
Let us introduce the following relevant frequencies. In chapters 4 and 5 the origin of these frequency components and spectra will be explained.

- chirp start frequency: $f_{IF1} = DC = 0 \text{ Hz}$,
- chirp stop frequency: $f_{IF2} = 8 \text{ MHz}$,
- system clock of the DDS: $f_{REFCLK} = 400 \text{ MHz}$,
- low-pass filter stop frequency at 3 dB attenuation: $f_{3dB} = 70 \text{ MHz}$,
- local oscillator (LO) frequency: $f_{LO} = 5.3 \text{ GHz}$,
- harmonics of the LO: $n \times f_{LO} = n \times 5.3 \text{ GHz}$ with $n \in \mathbb{N}$,
- intermodulation products due to the frequency translation of the mixer:
 $n \times f_{LO} + m \times f_{IF} = n \times 5.3 \text{ GHz} + m \times 8 \text{ MHz}$ with $n, m \in \mathbb{N}$.

In Table 3.1 an overview of the frequency components and the spectra is shown. The drawn spectrum schemes are not scaled: the height of the components should only give a rough estimation of the amplitude and the frequency marks are placed to get a general idea of the spectrum at the output of the component.

¹The noise figure is clearly a more important issue for a receiver front-end because in that case it is indispensable to amplify very weak signals with a low SNR in a low-noise first stage. For the case of a transmitter using the LNA is rather a “best choice” option.

Table 3.1: Frequency budget of the transmitter along the subsystems

| Component | Frequency Operation | Spectrum Scheme |
|-----------------------------|---|---|
| Direct Digital Synthesizer | generating a chirp signal: $f_{IF1} \leftrightarrow f_{IF2}$ |  |
| Low-Pass Filter | filtering out frequency components higher than the 3dB- stop frequency f_{3dB} |  |
| Local Oscillator | generating one frequency component at f_{LO} (side effect: harmonics at $n \times f_{LO}$), $n > 1$ |  |
| Wilkinson Quadrature Hybrid | / |  |
| Mixer | upconverting to a chirp signal: $f_{LO} \pm f_{IF1} \leftrightarrow f_{LO} \pm f_{IF2}$ |  |
| Wilkinson Power Combiner | eliminating one side band, e.g. the lower side band: $f_{LO} + f_{IF1} \leftrightarrow f_{LO} + f_{IF2}$ |  |
| Low-Noise Amplifier | / |  |
| Band-Pass Filter | filtering out harmonics of the LO at $n \times f_{LO}$ |  |
| Power Amplifier | 27 / |  |

Notice that although the Wilkinson power combiner does not change the frequency directly, by combining the in-phase and quadrature frequency components from both its inputs, one frequency side band is significantly attenuated (theoretically even eliminated, as was previously explained in section 3.1.2). The Wilkinson quadrature hybrid, the low-noise amplifier and power amplifier do not really change the frequency spectrum –the phase on the contrary is changed by the quadrature hybrid– and theoretically only amplify or attenuate the frequency components of their input spectra. This means that they will not introduce any frequency conversion. This is indicated as a “/”-sign in Table 3.1 to give a clear overview.

3.1.5 Power Budget

To acquire the transmitted signal at the receiver with a sufficient Signal-to-Noise Ratio (SNR), a constraint was set up for the output signal power of the transmitter which is realized through this project. This signal power should be about 10 dBm or more (with a tolerance of a few dB’s).

The design of the transmitter is obviously done before the simulations, therefore the losses from the filters were approximated (based on similar filter designs) and the gain values from the data sheets will certainly not exactly be equal to the measured values at the end of the project. But this approximation is defensible because it tells at least if the transmitter is realizable for the given specifications.

In Table 3.2, an approximate power budget along the transmitter subsystems is showed:

Table 3.2: Power budget of the transmitter along the subsystems

| Component | Gain (dB) | Component Gain (dB) |
|----------------------------|---------------------------|---------------------|
| Direct Digital Synthesizer | / | -7 (given) |
| Low-Pass Filter | +/- 0 (approximation) | -7 |
| Mixer | -8 (cf. data sheet) | -15 |
| Wilkinson Power Combiner | -3 (per input, Ref. [11]) | -18 |
| Low-Noise Amplifier | +11 (cf. data sheet) | -7 |
| Band-Pass Filter | -3 (approximation) | -10 |
| Power Amplifier | +19 (cf. data sheet) | 9 |

3.1.6 Phase Noise

There are two dominating sources of phase noise in the test transmitter: the local oscillator and the direct digital synthesizer (DDS).

For the local oscillator, the phase noise values of the HP 8340B synthesized sweeper with output frequency between 2.3 GHz and 7 GHz are given in its data sheet and in Table 3.3:

Table 3.3: Single side band phase noise of the HP 8340B synthesized sweeper

| Offset from carrier | Single side band phase noise (dBc/Hz) |
|---------------------|---------------------------------------|
| 30 Hz | -64 |
| 100 Hz | -70 |
| 1 kHz | -78 |
| 10 kHz | -86 |
| 100 kHz | -107 |

For the DDS, the phase noise values of the AD9954 DDS with output frequency 9.5 MHz are given in its data sheet, and in Table 3.4:

Table 3.4: Single side band phase noise of the AD9954 DDS

| Offset from carrier | Single side band phase noise (dBc/Hz) |
|---------------------|---------------------------------------|
| 10 Hz | -100 |
| 100 Hz | -110 |
| 1 kHz | -120 |
| 10 kHz | -130 |
| 100 kHz | -140 |
| 1 MHz | -145 |

We can then do an estimation of the phase noise power by integrating these values over their frequency interval (difference between two adjacent frequency offsets).

This gives a phase noise power of -33.6 dBc or a phase error of 0.02 radians for the local oscillator. And for the DDS, this gives a phase noise power of -73.1 dBc or a phase error of 0.0002 radians.

It is clear that the phase error of the DDS is negligible compared to the phase error of the local oscillator: this latter one will dominate the phase noise of the entire transmitter circuit. This phase error, which is 0.02 radians, should then be compared to the phase error of the existing transmitters of opportunity. This phase error was derived in section 3.1.1, and with the expected error of 0.1 radians it was an order of magnitude higher than the one derived in this section for the test transmitter. This means that the test transmitter is realizable for the given phase noise specifications.

3.1.7 Substrate Characteristics

The microstrip line width depends on the thickness of the substrate and the substrate has to be chosen in function of the frequency band too. At the RF

lab of Universitat Politècnica de Catalunya (UPC), department of Signal Theory and Communications (TSC) the laminate or substrate with the following characteristics is used. Why this substrate is convenient will become clear in the next chapters.

- Rogers RO4003 (data sheet at Ref. [4]), with a
- substrate thickness H of 0.8 mm,
 - substrate relative dielectric constant ε_r of 3.55 (recommended value for design, theoretical value $\varepsilon_r = 3.38$),
 - relative permeability μ_r of 1,
 - upper ground plane to substrate spacing of 1 m,
 - conductor thickness T of $35 \mu m$,
 - conductor conductivity of 60×10^6 ,
 - dielectric loss tangent of 0.0027,
 - RMS surface roughness of $0.4 \mu m$.

3.2 Simulation & Layout Tools

Now that is known from section 3.1 what will have to be simulated and what layout should be done, it will be explained what software tools have been used to do this in an efficient way.

- Agilent’s Advanced Design System, further mentioned as “ADS”, is “a powerful electronic design automation software system. [...] Advanced Design System is the industry leader in high-frequency design. [...] With a complete set of simulation technologies ranging from frequency-, time-, numeric and physical domain simulation to electromagnetic field simulation, ADS lets designers fully characterize and optimize designs. The single, integrated design environment provides system, circuit, and electromagnetic simulators, along with schematic capture, layout, and verification capability, eliminating the stops and starts associated with changing design tools in mid-cycle” (Ref. [5]).

Most of the subsystems of the transmitter are linear passive circuits and do not need to be tested for nonlinearities: an S-parameter simulation would be sufficient which is perfectly possible with ADS. But even then, to simulate the nonlinearities of the mixer, a harmonic balance simulation can be used as this is a frequency-domain analysis technique specifically for simulating distortion in nonlinear circuits and systems. Moreover, the design of the transmitter should not be optimized to obtain the best product on the market: a working transmitter would satisfy the needs for testing purposes and in the end for example, a few more dB’s of insertion loss are still acceptable.

- Agilent’s Momentum, further mentioned as “Momentum”, is “a part of ADS. [...] It is a 3D-planar electromagnetic (EM) simulator that computes S-parameters for general planar circuits, including microstrip, slotline, stripline, coplanar waveguide, and other topologies. [...] Momentum gives you a complete tool set to predict the performance of high-frequency circuit boards, antennas, and ICs by accurately simulating complex EM effects including coupling and parasitics” (Ref. [5]).

This part of ADS is very useful to verify the preliminary simulation results done with ADS’ circuit simulator and to improve passive circuit performance in a final step before starting the layout. It increases confidence that the manufactured product will function as simulated.

- Agilent’s LineCalc, further mentioned as “LineCalc”, is a part of ADS. It is “an analysis and synthesis program for calculating electrical and physical parameters of single and coupled transmission lines” (Ref. [5]).

For the layouts of the IQ modulator the line width is calculated for microstrip lines.

For the low-noise amplifier and power amplifier the line width is calculated for coplanar waveguide with back ground plane².

²The reason why the low-noise amplifier and the power amplifier are calculated for coplanar

- Agilent’s Design Assistant, further mentioned as “Design Assistant”, is a part of ADS. It is “used to generate and update the design contained for example within a single passive circuit from the given specifications” (Ref. [5]).
- CadSoft’s EAGLE, further mentioned as “EAGLE”, is “an easy to use, yet powerful tool for designing printed circuit boards (PCBs). The name EAGLE is an acronym, which stands for Easily Applicable Graphical Layout Editor” (Ref. [3]). The engineers of CadSoft have more than 15 years of experience and over 20000 users, including corporations like AMD, Hewlett-Packard, Nokia, Philips, NASA, IBM, Intel and the department TSC of Universitat Politècnica de Catalunya (UPC) are using this software.

EAGLE was used for all layouts in this project rather than the ADS layout editor because it provides many tools and libraries that are either more complicated to use or simply unavailable in ADS. Moreover, there is a free light version with only a few limitations (limited board size and number of layers).

waveguide with back ground plane is explained in section 5.6.

Chapter 4

Base Band Subsystems

4.1 Direct Digital Synthesizer

Although there exists a complete quadrature Direct Digital Synthesizer (DDS) module (model AD9854 from Analog Devices) which outputs an in-phase and quadrature signal modulator, it was chosen for two DDS's of model AD9954 which then had to be synchronized and shifted 90 degrees in phase with respect to each others outputs. This choice was made because a PCB board which was programmed to steer one of both DDS's already was available in the TSC lab. This model also produces a very low phase noise –just like the AD9854 does– which is certainly less than the oscillator will produce¹ and therefore it is suitable.

In Figure 4.1 the block diagram of the DDS is showed.

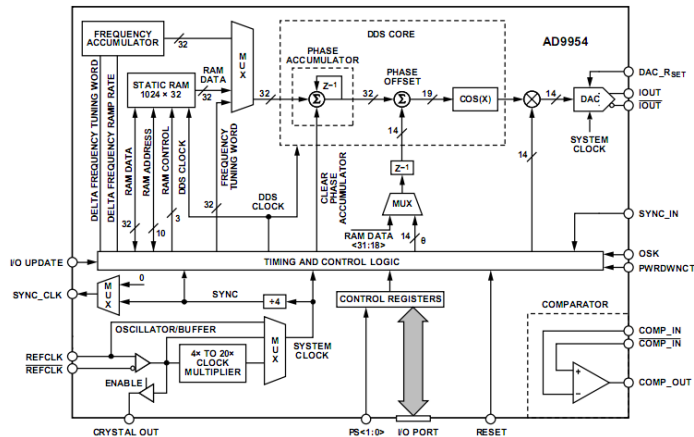


Figure 4.1: Block diagram of the DDS AD9954

To program the control registers of the AD9954 DDS, we use the Spartan-3 Field-Programmable Gate Array (FPGA) XC3S100E, manufactured by Xilinx (Ref. [15]). The FPGA was chosen for its very low cost and high-performance logic for high-volume consumer-oriented applications compared to an application-specific integrated circuit (ASIC). Moreover, the Picoblaze KCPSM3² 8-bit Micro Controller inside the FPGA offers a programmable state machine. To do so, it only uses a small amount of logic (96 Spartan-3 slices or +/- 10% of the XC3S100E device) and a single block RAM to form a ROM store for a program of up to 1024 instructions.

In Figure 4.2 the board with two DDS's (on the picture: number 4) and the FPGA (number 3) is shown. The outputs of the DDS's are then matched

¹Although a mobile oscillator will be used in practical transmission tests, the phase noise of the heavy but better performing synthesizer HP 8340B still has a phase noise which will dominate in the transmitter circuit. This was calculated in section 3.1.6.

²(K)constant Coded Programmable State Machine.

to $50\ \Omega$ and followed by the low-pass filter (number 5) which will be discussed in section 4.2. To provide the DDS system clock at 20 MHz, the REF OUT signal of the Spectrum Analyzer, which is a sine wave with frequency 10 MHz, is used and connected to a 2x frequency multiplier (number 1). With a splitter (number 2) the same clock is provided to the upper DDS (number 4) and the lower DDS.

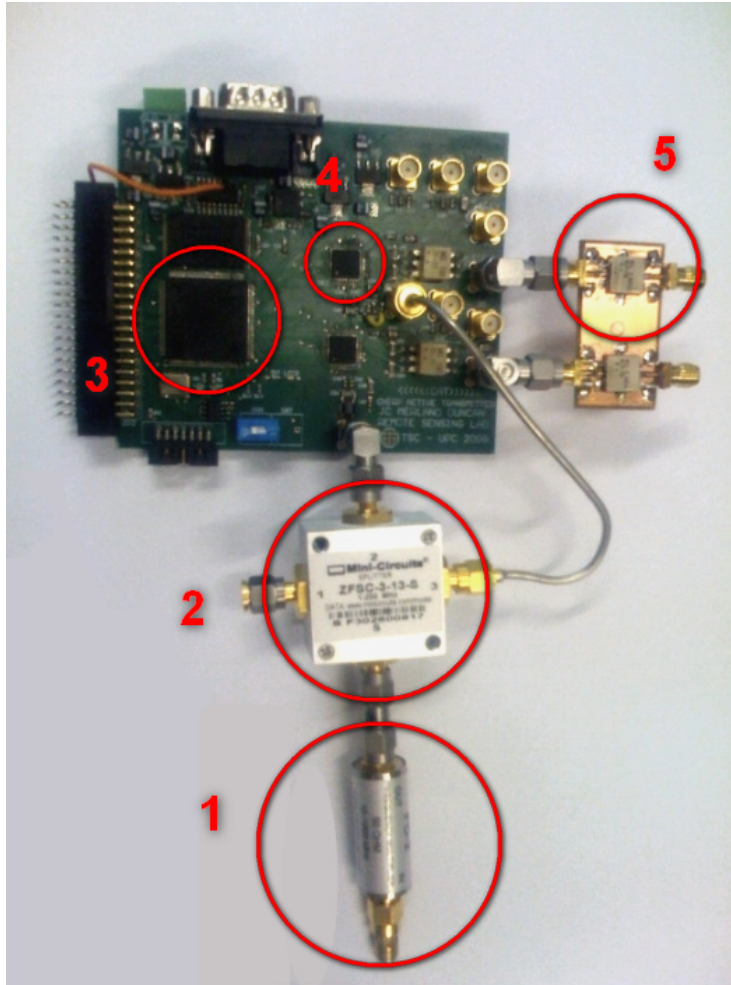


Figure 4.2: Picture of the FPGA, the two DDS's and the low-pass filter

The registers of the DDS have to be configured correctly as these determine the operation mode and parameters. In our case the following registers (with abbreviation and address) are applicable:

- Control Function Register No. 1 (CFR1) (at address 0x00): to control the various functions, features and modes of the AD9954,

- Control Function Register No. 2 (CFR2) (at address 0x01): to control the various functions, features and modes of the AD9954, primarily related to the analog sections of the chip,
- Frequency Tuning Word (FTW0) (at address 0x04): a 32-bit register that controls the rate of accumulation in the phase accumulator of the DDS core,
- Phase Offset Word (POW0) (at address 0x05): a 14-bit register that stores a phase offset value,
- Frequency Tuning Word (FTW1) (at address 0x06): a 32-bit register that sets the upper frequency in a linear sweep operation,
- Negative Linear Sweep Control Word (NLSCW) (at address 0x07): contains a 32-bit delta frequency tuning word (FDFTW and RDFTW) and an 8-bit sweep ramp rate word (FSRRW and RSRRW),
- Positive Linear Sweep Control Word (PLSCW) (at address 0x08): contains a 32-bit delta frequency tuning word (RDFTW) and an 8-bit sweep ramp rate word (RSRRW).

The following registers should not be cared about as the signal can be constant in amplitude:

- Amplitude Scale Factor (ASF) (at address 0x02): stores the 2-bit auto ramp rate speed value and the 14-bit amplitude scale factor used in the output shaped keying (OSK) operation,
- Amplitude Ramp Rate (ARR) (at address 0x03): stores the 8-bit amplitude ramp rate used in the auto-OSK mode.

To obtain a linear sweep which rises from DC to 8 MHz and immediately falls back from 8 MHz to DC again, like in Figure 4.3, we should also consider configuring the Linear Sweep No-Dwell bit. For synchronization the Automatic Synchronization Enable bit and the Autoclear Phase Accumulator bit are important. In the following is explained what these bits do:

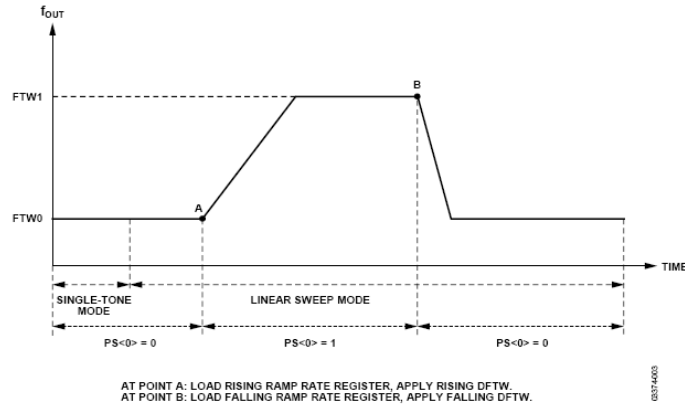


Figure 4.3: Linear sweep frequency plan

4.1.1 Linear Sweep Mode

To activate the linear frequency sweep mode, bit $\text{CFR1}\langle 21 \rangle$ should be set.

Moreover, bit $\text{CFR1}\langle 2 \rangle$ should be cleared because then the linear sweep no-dwell function is inactive. If the no-dwell mode is inactive when the sweep completes, sweeping does not restart until an I/O update or change in profile initiates another sweep. The output frequency holds at the final value in the sweep, although in our case input signal $\text{PS}\langle 0 \rangle$ will be set during exactly the time that the frequency needs to increase until the end frequency of 8 MHz (see Figure 4.3). At that moment $\text{PS}\langle 0 \rangle$ is cleared and the frequency decreases to DC again.

If bit $\text{CFR1}\langle 2 \rangle$ would be set, the phase would be cleared when the sweep completes and the output frequency would almost immediately fall back to DC until another sweep is initiated via an I/O update input or change in profile.

4.1.2 Automatic Synchronization of both DDS's

To synchronize both DDS's, one should be configured as a master and the other is slaved to this master. The slave DDS then automatically synchronizes its internal clock to the SYNC_CLK output signal of the master device. To activate the automatic synchronization feature for the slave DDS, bit $\text{CFR1}\langle 23 \rangle$ should be set. This is not applicable for the master DDS.

4.1.3 Frequency Sweep

The output frequency (f_o) of the DDS is a function of the frequency of the system clock (SYSCLK), the value of the frequency tuning word (FTW), and the capacity of the phase accumulator (2^{32} , in this case). The exact relationship is given below with f_s defined as the frequency of SYSCLK :

$$f_O = \frac{(FTW)(f_S)}{2^{32}} \text{ with } 0 \leq FTW \leq 2^{31} \quad (4.1)$$

$$f_O = f_S \times \left(1 - \left(\frac{FTW}{2^{32}}\right)\right) \text{ with } 2^{31} < FTW < 2^{32} - 1 \quad (4.2)$$

In the Linear Sweep Mode going from 0 MHz to 8 MHz, FTW0 and FTW1 are found to be, with the first equation:

$$FTW0 = (f_O)/(f_S) \times 2^{32} = \frac{0 \text{ MHz}}{400 \text{ MHz}} \times 2^{32} = 0 \times 00000000 \quad (4.3)$$

$$FTW1 = (f_O)/(f_S) \times 2^{32} = \frac{8 \text{ MHz}}{400 \text{ MHz}} \times 2^{32} \approx 85899346 = 0 \times 051EB852 \quad (4.4)$$

4.1.4 Quadrature Phase Offset

As we are programming the DDS to maintain a static output phase, the primary method of setting the POW is by programming the desired value into the POW0 register.

The phase offset formula is

$$\Phi = \frac{POW}{2^{14}} \times 360^\circ \quad (4.5)$$

As we need 90° phase offset for the DDS which sends the quadrature signal, POW should be 2¹² or 0x1000 or POW0 < 12 > = 1 and all other bits of POW0 should be cleared.

For the DDS which sends the in-phase signal, POW should be 0 or POW0 < 12 > = 0 and all other bits of POW0 should also be cleared.

4.1.5 Clear the Phase Accumulator

Each time a new I/O update is sent, the phase accumulator adds the phase of the signal to the phase stored in the control register (POW0 of section 4.1.4) and the phase of the previous I/O update (see Figure 4.1). This means that if we do not clear the phase accumulator at every I/O update, the phase would be accumulating in an uncontrolled manner, in this way not outputting the desired chirp signal with an offset phase of 0 or 90 degrees.

Therefore, the Autoclear Phase Accumulator bit CFR1<13> has to be set: the phase accumulator is automatically and synchronously cleared for one cycle upon receipt of an I/O update signal.

4.1.6 Measurements

To check if both in-phase and quadrature signals at the output of the DDS were synchronized and shifted 90 degrees in phase as was configured in the control registers, the digital real-time oscilloscope TDS 210 was used.

First a singletone of $\pm 24\text{ MHz}$ was configured to compare both output signals and the satisfying result is shown in Figure 4.4. The peak-to-peak voltage of these signals is about 80 mV, or about -7 dBm power (for a load of $50\ \Omega$) which confirms the value given in section 3.1.5.

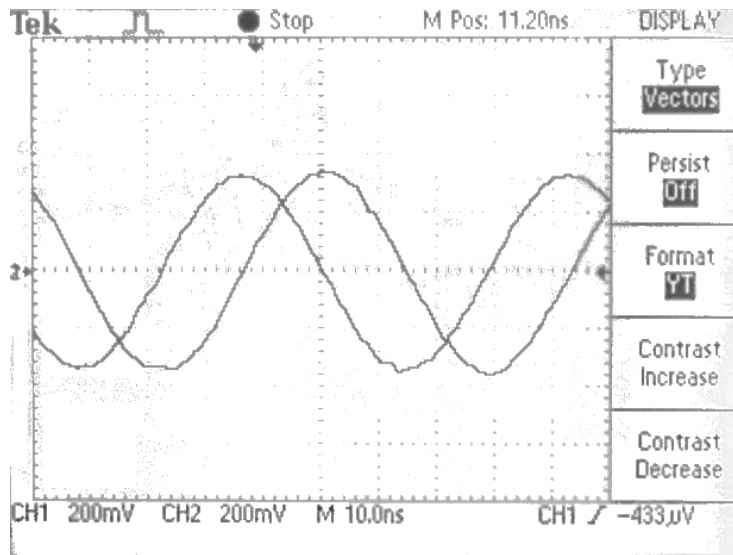


Figure 4.4: DDS singletone in-phase and quadrature output versus time

If both output signals were perfectly in-phase and synchronized, the measurement of one output signal (e.g. quadrature) versus the other output signal (e.g. in-phase) should be a perfect circle. This can be easily seen: let's say that the in-phase signal is $x = \sin(\omega t)$, on the abscissa, and the quadrature signal is $y = \cos(\omega t)$, on the ordinate. As one knows, $[\cos(\omega t)]^2 + [\sin(\omega t)]^2 = 1$ counts and $x^2 + y^2 = 1$ is also the equation of a circle with radius 1 and centered around the origin. The result is shown in Figure 4.5. The small line off the circle shows that the two DDS's are not completely synchronized at that time; this could be at the moment that PS<0> switches to start a frequency ramp in the opposite direction. But as it represents only a very short period of time –most of the time the circle is followed which results in a thick circle– it is acceptable.

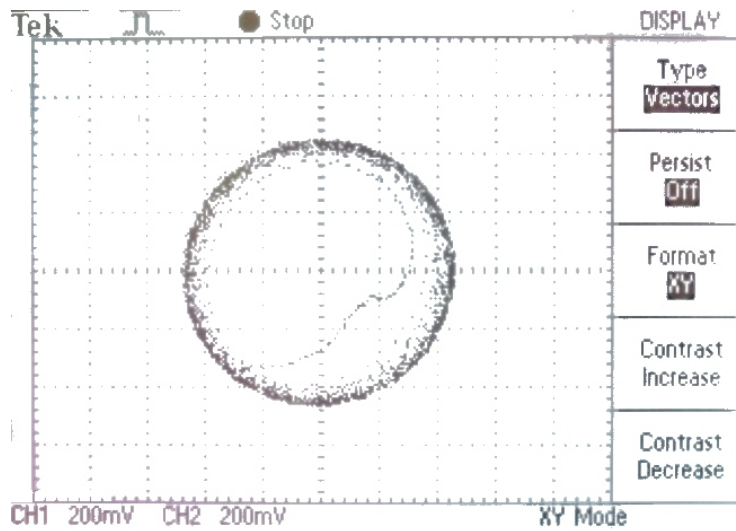


Figure 4.5: DDS chirp in-phase output versus quadrature output

The in-phase and quadrature chirp signals at the output of the DDS were also both sampled and digitized, then read out with MATLAB. The result is shown in Figure 4.6 with the amplitude versus time.

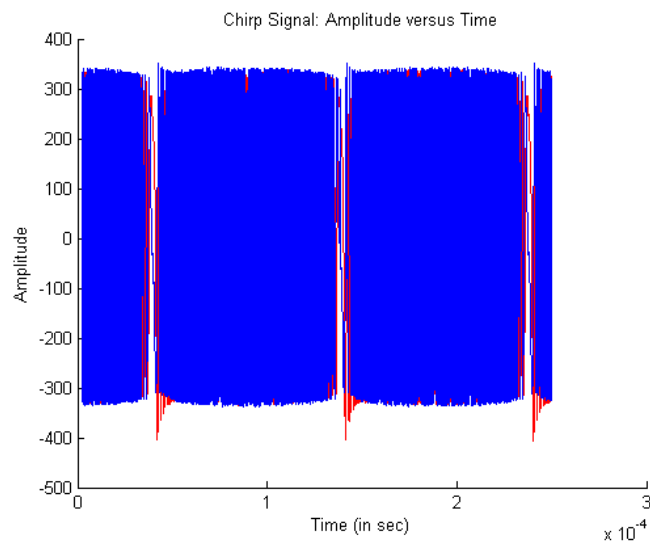


Figure 4.6: DDS chirp output signal: amplitude versus time

By using the command `fft()` Figure 4.7 and Figure 4.8 were constructed,

the first showing the spectrum of the chirp signal between -8 and 8 MHz and the second showing the frequency sweep plan in time.

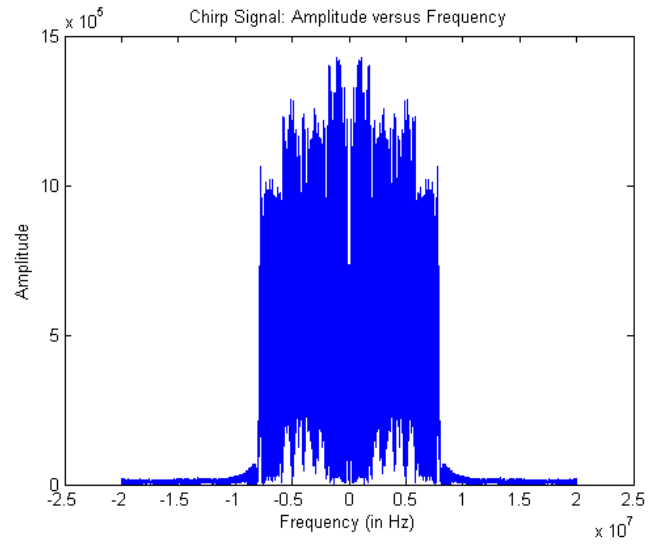


Figure 4.7: DDS chirp output signal: amplitude versus frequency

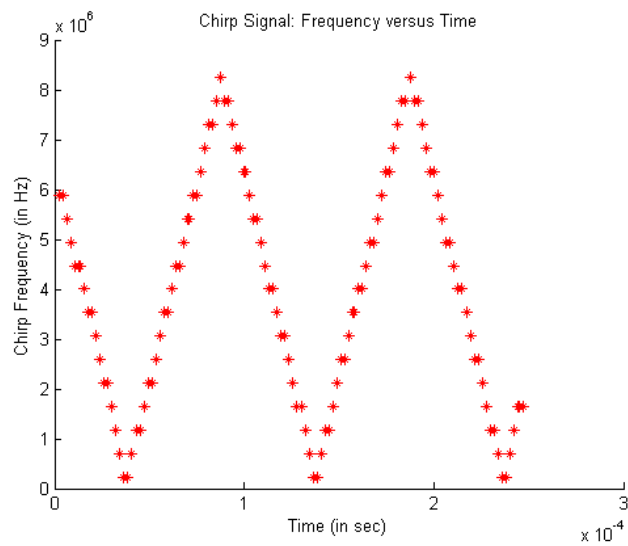


Figure 4.8: DDS chirp output signal: frequency versus time

Finally the DDS output was also measured with the spectrum analyzer and

this is shown in Figure 4.9. This figure can be compared to Figure 4.7, which was calculated with MATLAB. Of course only the positive frequencies are visible as negative frequencies are a purely theoretical concept.

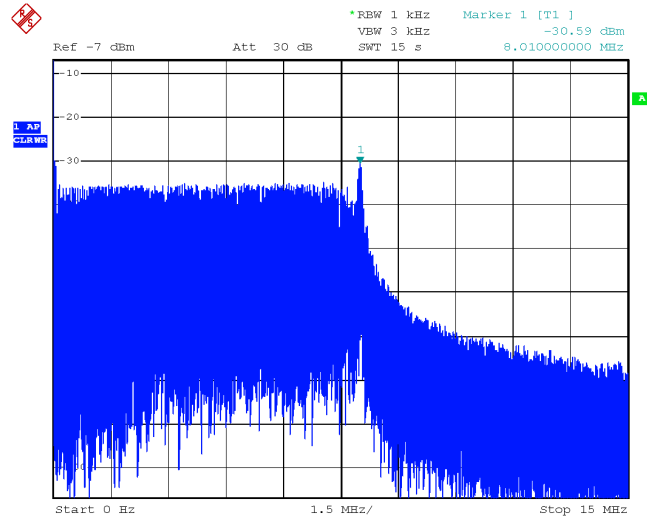


Figure 4.9: DDS chirp output signal measured with the spectrum analyzer

4.2 Low-Pass Filter

The purpose of this filter is to filter out the reference or system clock of the DDS (REF_CLK or SYS_CLK) at 400 MHz which may certainly not be upconverted by the mixers (see Figure 4.10). Therefore it should have a bandwidth of roughly 100 MHz and attenuate more than 60 dB at 400 MHz.

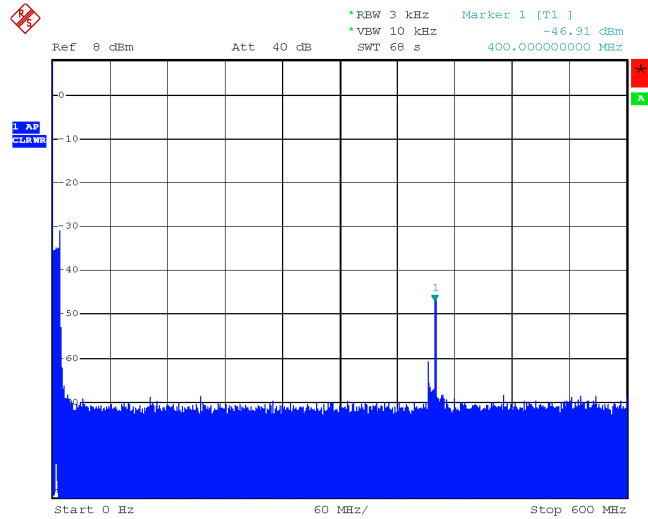


Figure 4.10: Output of the DDS with the system clock at 400 MHz

The data sheet of the AD9954 DDS proposes the elliptic low-pass filter³ shown in Figure 4.11, which is supposed to be good for a small ripple in the pass band (e.g. ± 0.2 dB) and a high selectivity⁴.

³Except for the circuit, no further details about the synthesis of this low-pass filter are given.

⁴The selectivity k is a measure for the steepness of the transition from pass band to stop band. The higher the selectivity of the filter, the more components are needed and the more difficult it is to realize the filter. This value lies between 0 and 1. In this case it can be calculated that $k = \frac{f_d}{f_s} \approx \frac{180 \text{ MHz}}{220 \text{ MHz}} = 0.82$ with f_d and f_s pass frequency and stop frequency respectively.

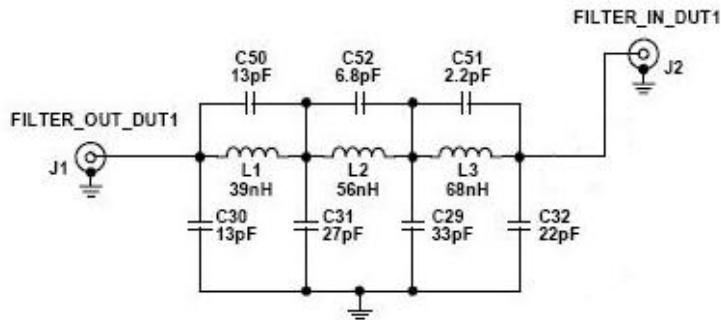


Figure 4.11: Low-pass filter proposed in the data sheet of the AD9954 DDS

But as another low-pass filter with a bandwidth of $\pm 70\text{ MHz}$, the RLP-70+ from manufacturer Mini-Circuits, was in stock in the TSC lab and that this filter could fulfill the same needs, this one was used. In Figure 4.12 the insertion loss of this filter is shown and it is clear that from 70 MHz and higher, the input signal will be attenuated. At 400 MHz an attenuation of at least 60 dB is expected.

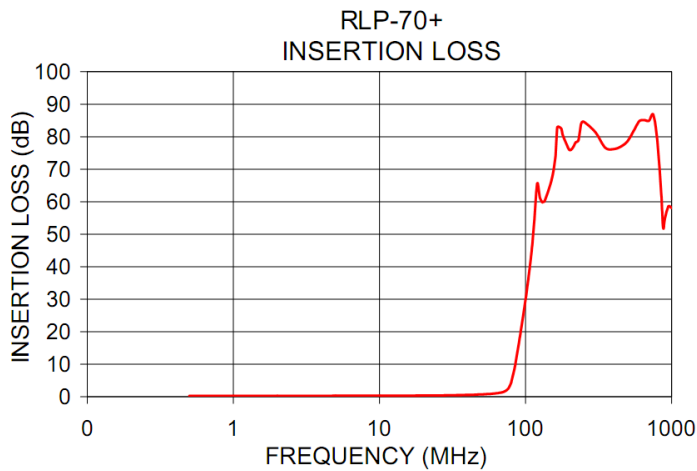


Figure 4.12: Insertion loss of the RLP-70+ low-pass filter (manufactured by Mini-Circuits)

After calibrating the Agilent Technologies N5242A PNA-X Network Analyzer, an S-parameter measurement was done and reflection coefficients S_{11} and S_{21} are shown in Figure 4.13. As we expected an attenuation at 400 MHz of around 70 dB is measured.

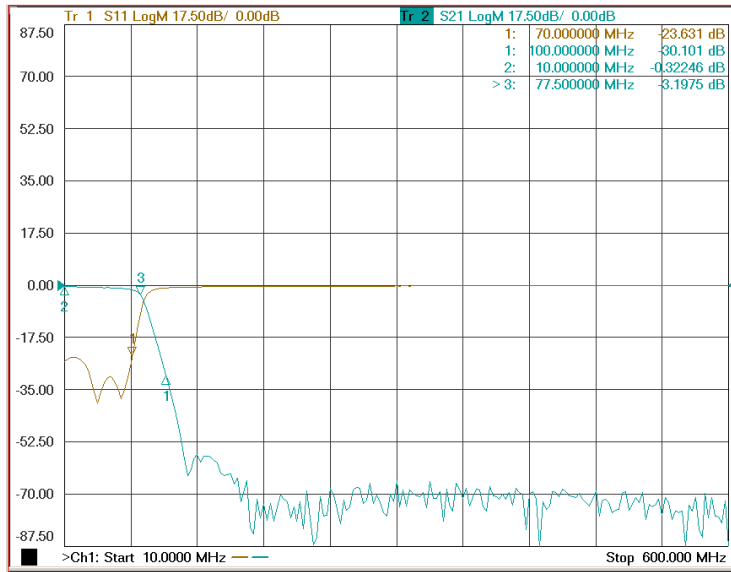


Figure 4.13: S-parameter measurement of the RLP-70+ low-pass filter with the PNA-X network analyzer

Chapter 5

High-Frequency Subsystems

5.1 Wilkinson Quadrature Hybrid

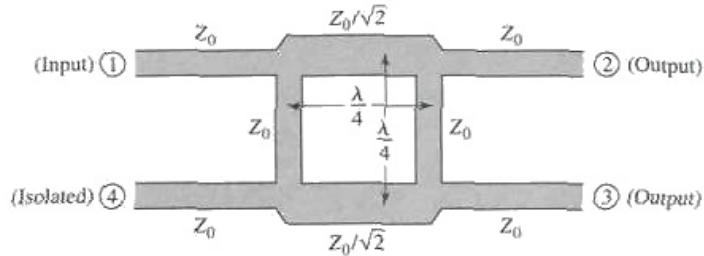


Figure 5.1: Wilkinson quadrature hybrid (Ref. [11])

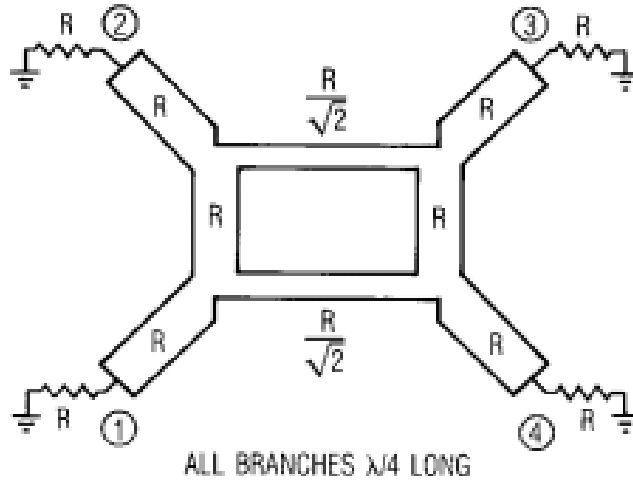


Figure 5.2: Wilkinson quadrature hybrid (Ref. [9])

To split the oscillator signal at the input in an in-phase signal and a quadrature signal at the output, i.e. two signals with equal frequency and amplitude but with a phase difference of 90 degrees, a Wilkinson quadrature hybrid (see Figure 5.1 and Figure 5.2) is used. This structure is also known as a branch-line hybrid (Ref. [9]). The basic operation of this hybrid is as follows: if all ports of Figure 5.1 are matched, then the input power at port 1 will be equally divided between port 2 and port 3, with the required 90 degrees phase shift between those two output ports. Theoretically no power should be coupled to port 4 but this is practically not possible due to all sorts of imperfections, e.g. design

approximations, material imperfections and manufacturing uncertainty should be considered. Note that port 4 is also terminated with a matched resistor.

As can be seen on the simulation result in Figure 5.3 a difference of only 0.082 dB between quadrature (S-parameter S_{31}) and in-phase (S-parameter S_{41}) outputs is simulated which is barely significant compared to the manufacturing uncertainty and therefore certainly acceptable.

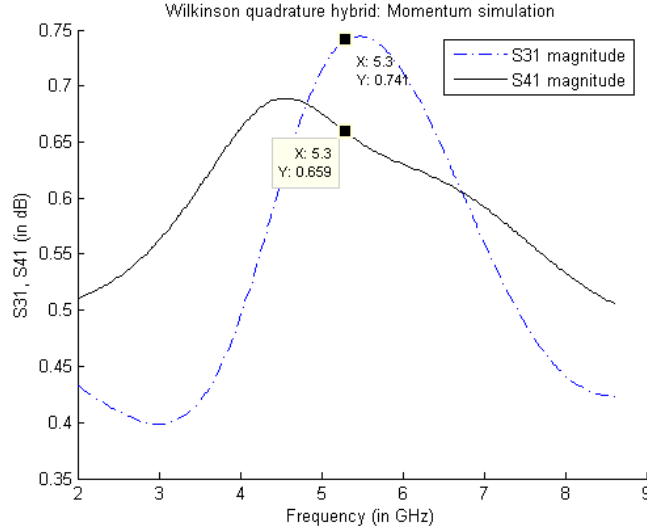


Figure 5.3: Insertion loss of in-phase (S_{41}) and quadrature (S_{31}) output compared

The line width W of a transmission line should be an order of magnitude smaller than the wavelength λ^1 (i.e., $W/\lambda < 0.1$) so that currents transverse to the microstrip line can be neglected (Ref. [1]). Therefore, the commonly used Rogers RO4003 substrate (Ref. [4]) at the VUB ELEC lab of 1.5 mm high is not advised (see Figure 5.4) as this results in $(W/\lambda)_{H=1.5\text{ mm}} = \frac{3.353\text{ mm}}{56.60\text{ mm}} = 0.06$ which is too close to the limit for $W/\lambda = 0.1$.

¹ $\lambda = \frac{c}{f} = \frac{3 \times 10^8 \text{ m/s}}{5.3 \times 10^9 \text{ Hz}} = 56.60 \text{ mm}$ with c : speed of light and f : frequency.

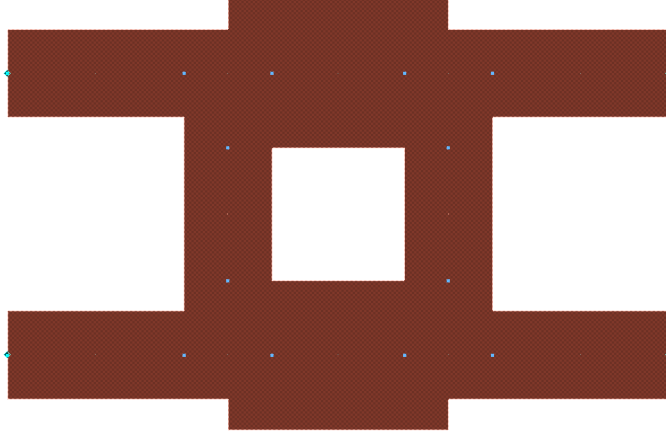


Figure 5.4: Wilkinson quadrature hybrid layout with substrate height $H = 1.5$ mm

Instead the thinner substrate with a thickness H of 0.5 mm could be used, or as commonly used at the TSC lab, the RO4003 substrate of $H = 0.8$ mm thick. This results in a W which is roughly 2 times smaller than for $H = 1.5$ mm, or $(W/\lambda)_{H=0.8\text{ mm}} = \frac{1.750\text{ mm}}{56.60\text{ mm}} = 0.03 \approx \frac{1}{2} \times (W/\lambda)_{H=1.5\text{ mm}}$.

It can be accepted in general that the height H varies with the microstrip width W .

Both substrates with $H = 0.8$ mm and $H = 0.5$ mm give quite similar results as can be seen in Figure 5.5: the layout with $H = 0.8$ mm (resp. 0.5 mm) only loses roughly 0.10 dB (resp. 0.15 dB) at the outputs.

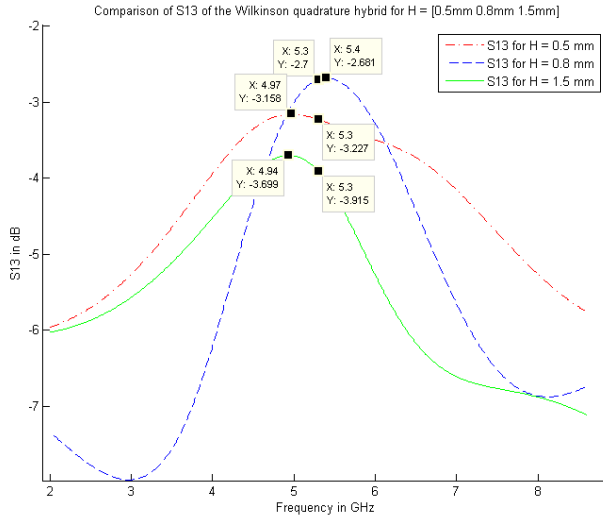


Figure 5.5: Simulation result of Wilkinson quadrature hybrid with $H = 0.8$ mm

The in-phase output is called LO_0deg and the quadrature output is called LO_90deg .

The $Z_0 = 50 \Omega$ lines and $\frac{1}{\sqrt{2}}Z_0 = 35.355 \Omega$ lines have to be calculated at 5.300 GHz. With LineCalc this gives 1.750 mm (or 68.879 mils) and 2.964 mm (or 116.680 mils) respectively.

The microstrip lines should be separated by $\frac{\lambda}{4}$ as shown in Figure 5.1. With LineCalc this gives 8.463 mm (or 333.178 mils). After optimization with Momentum, we obtain a phase difference closest to 90 degrees, if we use $\frac{\lambda}{4} = 9.163$ mm as can be seen in the variables attribution of Figure 5.6.

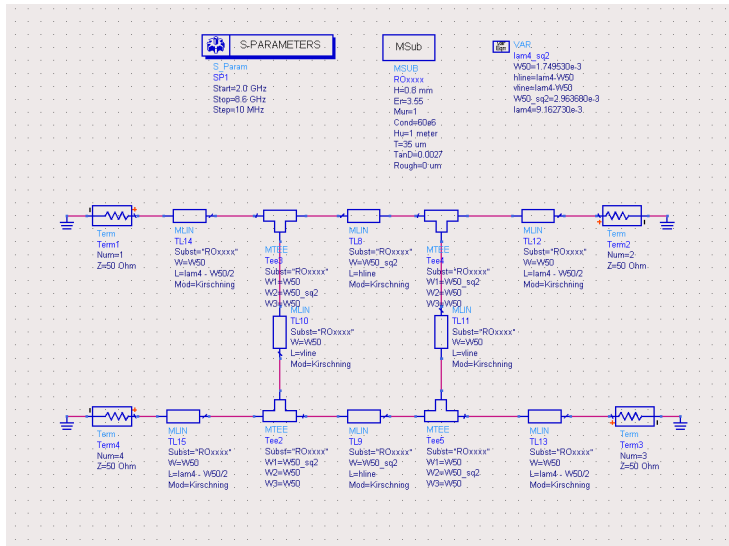


Figure 5.6: S-parameter simulation schematic of the Wilkinson quadrature hybrid, $\frac{\lambda}{4}$ (here called 'lam4') = $9.163 \times 10^{-3}m$

In Figure 5.7 we then see that at both ERS-2 and ENVISAT frequencies, the Momentum simulations result in a very satisfying phase difference of 89.95° and 89.89° respectively, but again these results are too precise in proportion to manufacturing uncertainty.

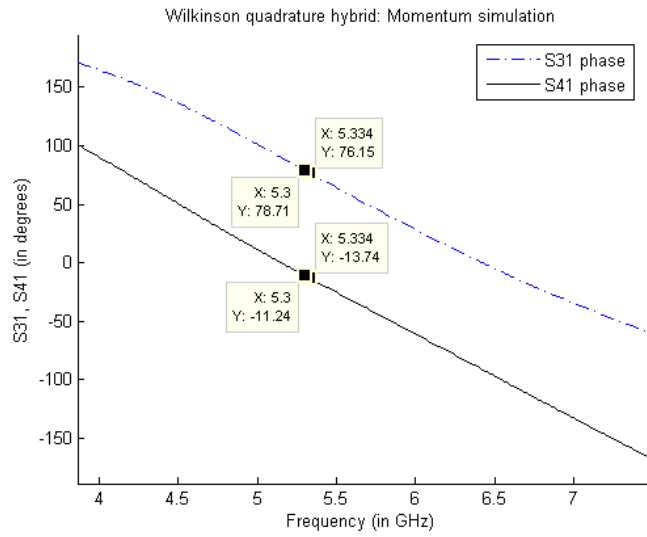


Figure 5.7: S-parameter simulation result with Momentum of Wilkinson quadrature hybrid

The layout of the hybrid is shown in the complete IQ modulator layout of section 5.4.

5.2 Mixer

5.2.1 Nonlinear Behaviour

The mixer that is being used is an upconverter mixer with component model HMC218, manufactured by Hittite Microwave Corporation and with package MS8. It is convenient for the SAR transmitter being built because it has a low conversion loss, high isolation, upconverts to RF frequencies between 4.5 and 6 GHz and has a sufficiently high input third-order intercept point (IIP3).

By convention the input ports are called the IF (Intermediate Frequency) port for base band (+/- 100 MHz) and the Local Oscillator (further mentioned as "LO") port (+/- 5.300 GHz); the output port is called the RF (Radio Frequency) port with a desired output at centre frequencies 5.300 GHz for ERS-2 and 5.331 GHz for ENVISAT.

The LO that is used in the TSC lab is the HP 8340B Synthesized Sweeper and it is set to deliver an output power of ± 10 dBm at the LO port whereas the Direct Digital Synthesizer (DDS) AD9954 (Analog Devices, Inc.) delivers an output power of -7 dBm at the IF port.

The mixer is the only component which could suffer from distortion due to nonlinearities because most of the other subsystems are linear and passive. That is why for the simulations ADS' harmonic balance simulation was used (see section 3.2). The input third-order intercept point (IIP3) is the specification which relates nonlinear third-order distortion products² to the linear (or first-order) term.

For every dB increase in input power, the third-order products will increase 3dB (see Figure 5.8). Or in other words, if we can decrease the linear term of the signal by 10 dB, we decrease the nonlinear third-order product of the signal by 30 dB which means we gained 20 dB's in linearity!

²The transfer function ($\frac{output}{input}$) can be modeled by a polynomial with Taylor series expansion.

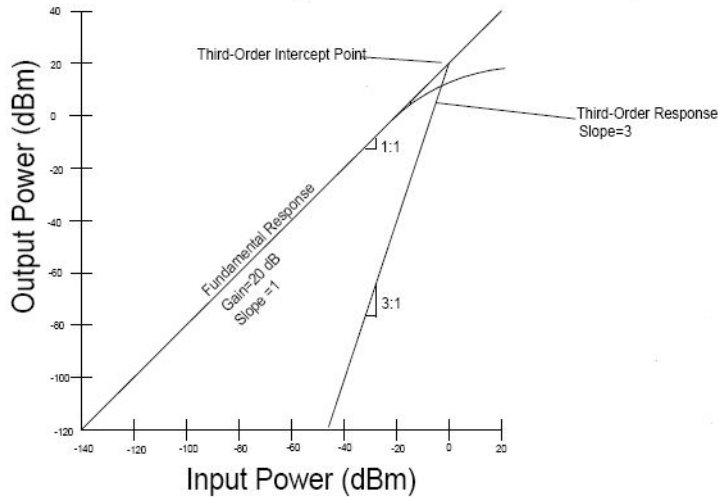


Figure 5.8: Third-order intercept point

The typical value of IIP3 (in dBm) of the HMC218 upconverter mixer for an LO frequency at 5.2 GHz is given in Table 5.1:

Table 5.1: Typical value of IIP3 of the HMC218 mixer (LO frequency at 5.2 GHz)

| LO input power (dBm) | IIP3 (dBm) |
|----------------------|------------|
| 7 | 12 |
| 10 | 14 |
| 13 | 16 |

We can conclude that for a sufficient LO input power, let's say 7 dBm + 2.7 dBm³, the IF input power of -7 dBm from the DDS is low enough to stay far from IIP3. As a result, the input of the mixer will be 19 dB lower than its IIP3 point (at 12 dBm). This assures that the higher-order nonlinear terms are small enough to be negligible. In this case they will appear approximately 2×19 dB or 38 dB below the signal power at the output which is an acceptable behaviour.

5.2.2 ADS Mixer Model

The S-parameters of the mixer are provided by the manufacturer: by interpolating the S_{33} reflection coefficient at the LO port – ($-S_{33}$) is also known as the

³The Wilkinson quadrature hybrid, which is the subsystem between the local oscillator (LO) and the LO-port of the mixer, has an insertion loss of about 2.7 dBm as seen in section 5.1.

LO return loss– is found to be $(-10.54, 81.79^\circ)$ at 5.300 GHz or by interpolation $(-10.71, 77.79^\circ)$ at 5.331 GHz, see Figure 5.9.

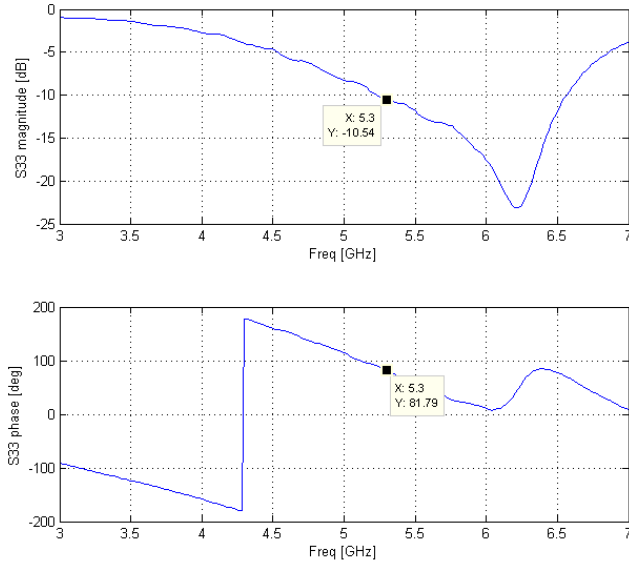


Figure 5.9: Reflection coefficient at LO-port of the HMC218 mixer

When simulating this mixer in ADS, isolated from the other components of the transmitter and matched at the output with a $50\ \Omega$ termination (see Figure 5.10), the power at the LO port gives an incorrect value of 20.460 dBm instead of the defined input power of 0 dBm (see Figure 5.11). As any possible feedback loops were excluded while still an additional 20.460 dBm of power coming from a possible incorrect mixer model was measured, it was decided to omit the LO return loss, i.e. $S_{33} = 0$ in all further simulations. Moreover, omitting this term didn't influence the loss terms of the adjacent stages.

Another explanation could be that the mixer was simulated with a too low LO input power. As said in section 5.2.1 the LO input power is preferably set to $\pm 10\text{ dBm}$ or more. This certainly has to be taken into account when testing the entire IQ modulator.

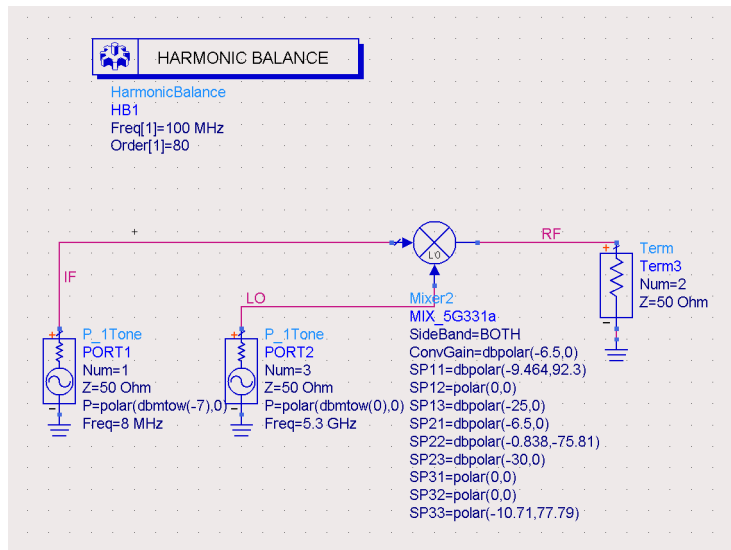


Figure 5.10: Harmonic balance simulation schematic of the HMC218 mixer

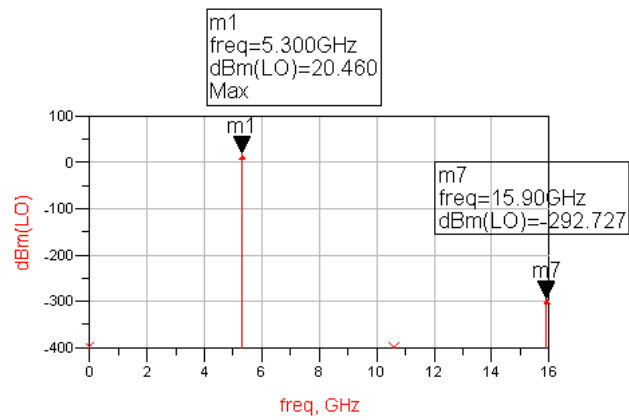


Figure 5.11: Harmonic balance simulation result of the HMC218 mixer

5.3 Power Combiner

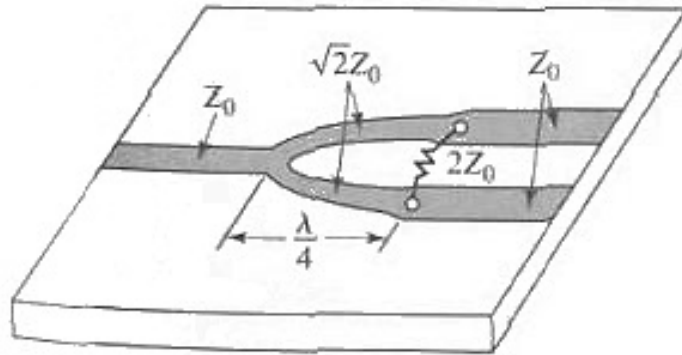


Figure 5.12: Wilkinson power divider (Ref. [11])

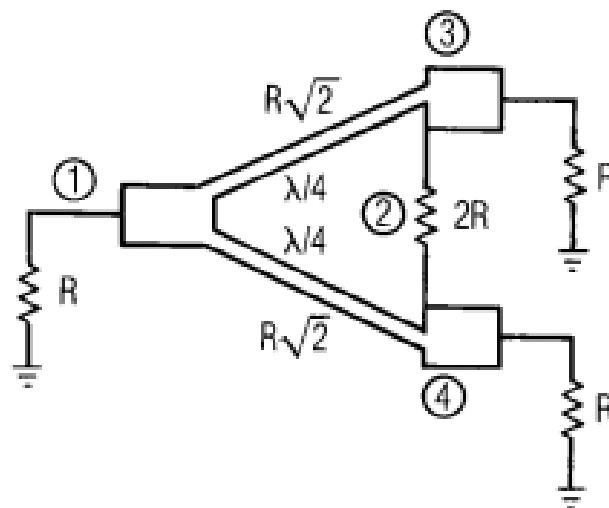


Figure 5.13: Wilkinson power divider (Ref. [9])

To combine both in-phase (I) and quadrature (Q) signals at the output of the two HMC218 mixers, a Wilkinson power divider (see Figure 5.12) is used in a reverse way, i.e. the two output ports are used as input ports and the input port

is used as the (combined) output port. This reversing can be done according to this line of reasoning:

The Scattering matrix S of the passive Wilkinson power divider is (Ref. [11]):

$$S = \frac{-j}{\sqrt{2}} \times \begin{bmatrix} 0 & 1 & 1 \\ 1 & 0 & 0 \\ 1 & 0 & 0 \end{bmatrix} \quad (5.1)$$

Now, assume that port 1 is the input of the divider, or the output of the combiner, then

$$\begin{bmatrix} b_1 \\ b_2 \\ b_3 \end{bmatrix} = \frac{-j}{\sqrt{2}} \times \begin{bmatrix} 0 & 1 & 1 \\ 1 & 0 & 0 \\ 1 & 0 & 0 \end{bmatrix} \begin{bmatrix} a_1 \\ a_2 \\ a_3 \end{bmatrix} \quad (5.2)$$

with a_i and b_i the incident and reflected power waves respectively ($i = 1, 2, 3$). For the power combiner the incident waves are a_2 and a_3 and port 1 is the output so, $a_1 = 0$ and a_2 should be equal to a_3 . This gives

$$b_1 = \frac{-1}{\sqrt{2}} \times (a_2 + a_3) \quad (5.3)$$

and the power at port 1 is then:

$$P_1 = \frac{1}{2} \times |b_1|^2 = \frac{1}{2} \times \frac{1}{2} \times (a_2^2 + 2 \times a_2 \times a_3 + a_3^2) \quad (5.4)$$

Now, if indeed $a_2 = a_3 = a$ and we write P_2, P_3 as the power at port 2 and port 3 respectively so that also $P_2 = P_3$, then the power at port 1 becomes:

$$P_1 = \frac{1}{2} \times \frac{1}{2} \times 4a^2 = a^2 = 2 \times P_2 = 2 \times P_3 = P_2 + P_3 \quad (5.5)$$

which is the function of a power combiner.

The Wilkinson power divider has the advantage to be matched at all ports and to have isolation between both output ports. Moreover, if both output ports are matched, the Wilkinson power divider theoretically is a lossless circuit, i.e. only reflected power is dissipated. As shown in Figure 5.13 another advantage is the fact that the 2R port termination does not need to be connected to ground.

In the given case, $R = Z_0 = 50 \Omega$. The microstrip lines with impedances $Z_0 = 50 \Omega$ and $\sqrt{2}Z_0 = 70.711 \Omega$ have to be calculated at 5.300 GHz. With LineCalc this gives respectively 1.750 mm (or 68.879 mils) and 0.932 mm (or 36.706 mils). Also, the microstrip lines should be separated by $\frac{\lambda}{4}$. With LineCalc this gives 8.463 mm (or 333.178 mils).

As described in Ref. [9] (pages 283-284) a $2Z_0 = 100 \Omega$ resistor is needed between both input ports of the power combiner as this forms two 50Ω terminations to the built-in 4th port like in the 180-degree hybrid. In this case, this port is not connected to ground. ADS Design Assistant designed a power

combiner with a gap of 1.25 mm which is 0.234 mm too large for the resistor with 0402 package (0.04 inches or 1.016 mm long) that is being used (see Figure 5.14). In all the following simulations, an extension of the microstrip line of 0.49 mm was taken into account to ease the soldering of the 100 Ω resistor because of the smaller gap of 0.27 mm (see Figure 5.15). On Figure 5.14 and Figure 5.15, the blue dots indicate inputs and outputs of all subcomponents (here: arced and T-form transmission line stubs) and the power combiner as an entity.

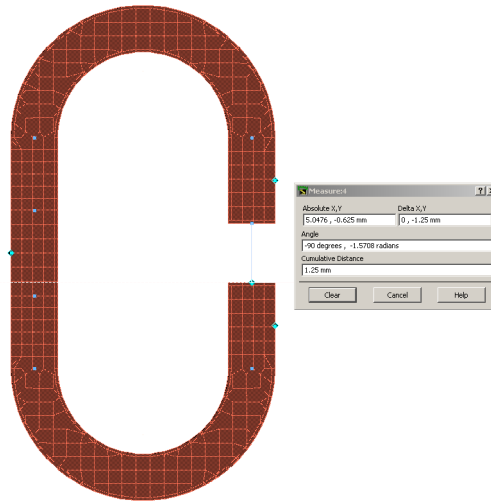


Figure 5.14: Gap for 100 Ω resistor, here 1.25 mm long

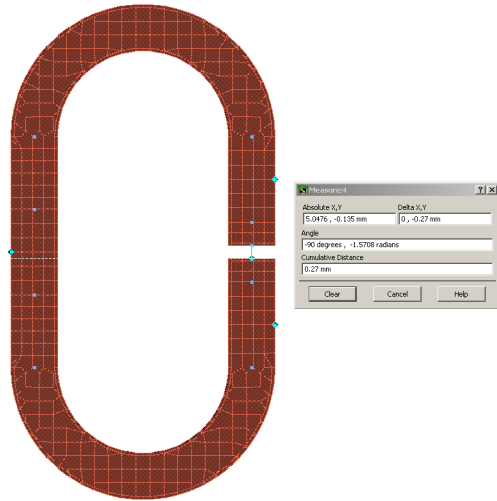


Figure 5.15: Gap for 100 Ω resistor, here 0.27 mm long

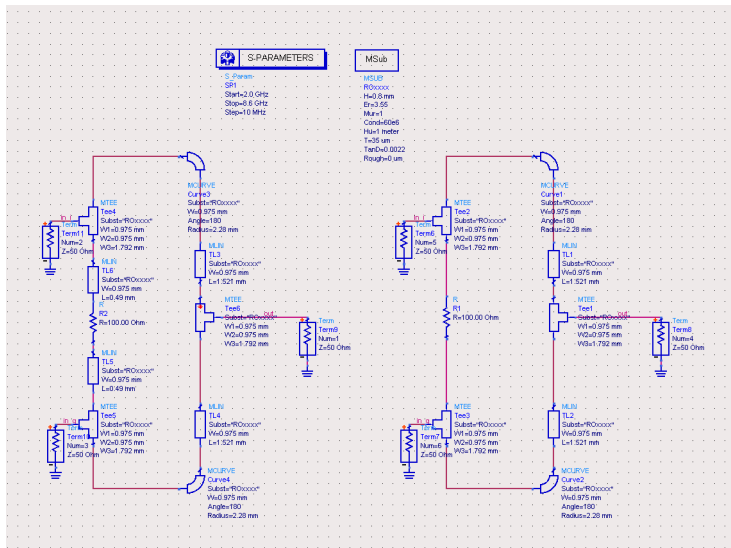


Figure 5.16: Simulation schematic of the Wilkinson power combiner; Left: with adaptation for too large gap and right: without adaptation

In Figure 5.16 the schematic is shown of the power combiner with adaptation for the too large gap (on the left), i.e. each side contains an additional microstrip line of 0.49 mm at the resistor to maintain symmetry, and without adaptation

(on the right). Notice that the circuit on the left defines input ports 2 and 3 and output port 1, and the circuit on the right defines input ports 5 and 6 and output port 4.

As can be seen from Figure 5.17 this barely influences the signal properties: the linear S-parameters from port 1 to port 2 and port 3 (S_{12} and S_{13} , or equally S_{21} and S_{31} for passive circuits) are equal at 5.300 GHz to the one from port 4 to port 5 and 6 (S_{54} and S_{64}).

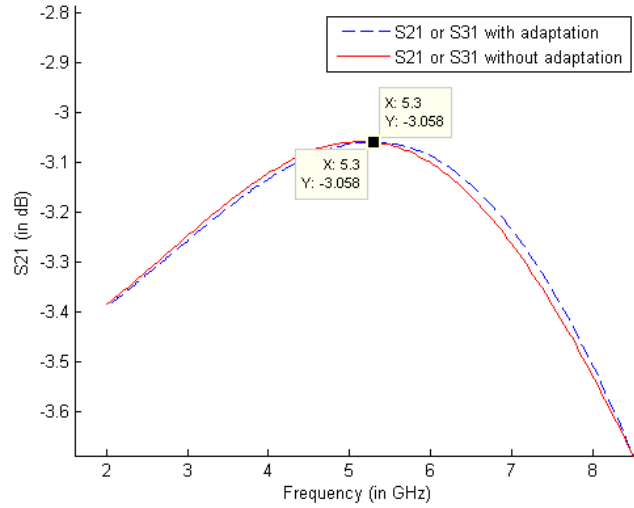


Figure 5.17: Comparison of S21 and S31 of the power combiner with and without adaptation

The S-parameter simulations are done with Momentum from 2.0 GHz to 8.6 GHz with centre frequency 5.300 GHz and frequency steps of 10 MHz for the adapted circuit (left on Figure 5.16). The substrate is given with the same characteristics as described in part Layout & Simulation Introduction.

As given in Ref. [11], the circuit is theoretically lossless so that we can expect the power at one of the inputs to be half of the power (or $10 \times \log_{10}(\frac{1}{2}) = -3 \text{ dB}$) at the output, and this is confirmed because as seen in Figure 5.17 the Momentum simulations expect an S-parameter of -3.058 dB at centre frequency 5.300 GHz. The simulated reflection coefficient S_{11} at the output port equals -21.670 dB at frequency 5.334 GHz, close to the previously mentioned centre frequency as seen in Figure 5.18.

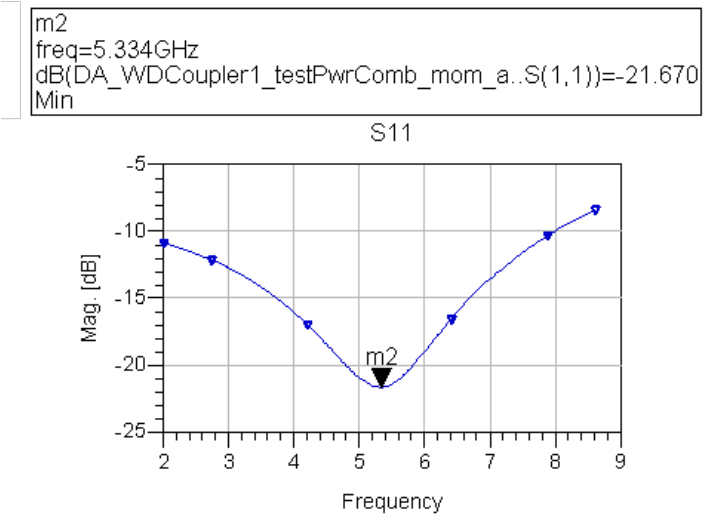


Figure 5.18: Minimal magnitude of S11 of the Wilkinson power combiner

5.4 IQ Modulator

In Figure 5.19 the schematic of the IQ modulator in EAGLE is shown.

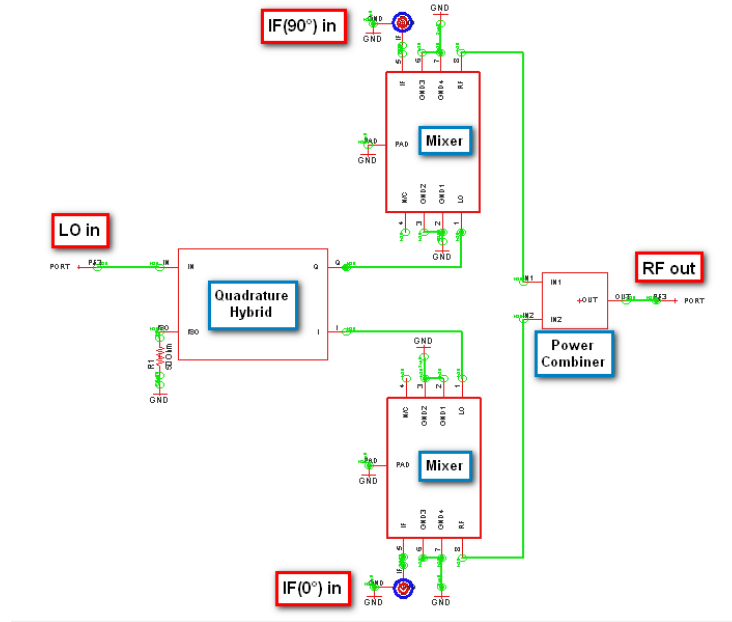


Figure 5.19: IQ modulator schematic in EAGLE

And in Figure 5.20 the layout of the IQ modulator in EAGLE is shown.

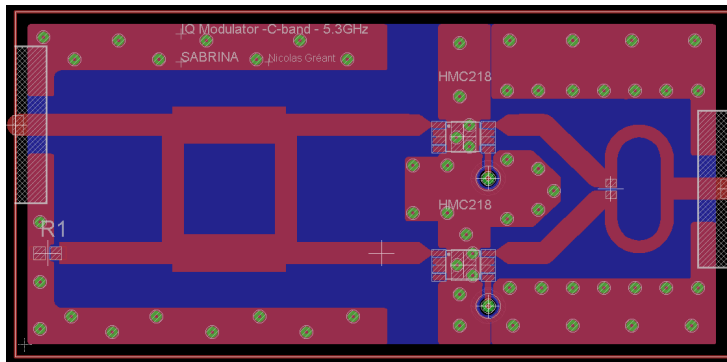


Figure 5.20: Layout of the IQ modulator, created with EAGLE

The Wilkinson quadrature hybrid together with the fact that the footprint of the mixers cannot be mirrored, introduce the asymmetry referred to the

horizontal axis in the layout, but from the two mixers on, every component or line should be as symmetric as possible to the vertical position of the output port.

When connecting each mixer RF port to each power combiner input port, we should choose the line with the least interference so the layout in Figure 5.20 is preferred over the layout in Figure 5.21.

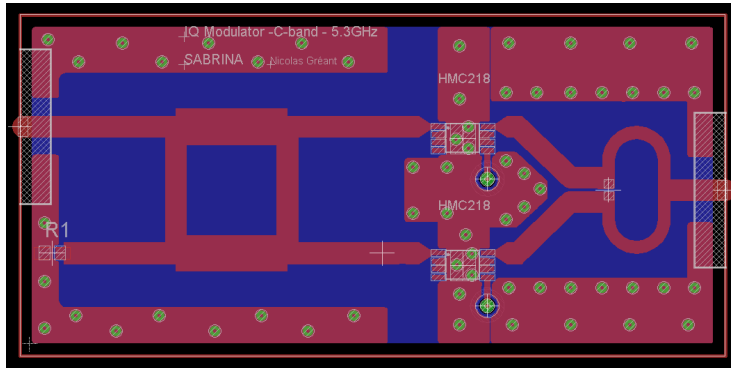


Figure 5.21: Bad example of placing two possibly interfering lines close to each other

As the IQ modulator should work for both ERS-2 and ENVISAT satellite signals with centre frequencies at 5.300 GHz and 5.331 GHz respectively, the simulations were done in Momentum and compared at both centre frequencies. The differences in insertion loss for the Wilkinson power combiner (see Figure 5.22) and Wilkinson quadrature hybrid (see Figure 5.23) are barely noticeable: maximum 0.005 dB of difference which is not significant in proportion to the manufacturing uncertainty!

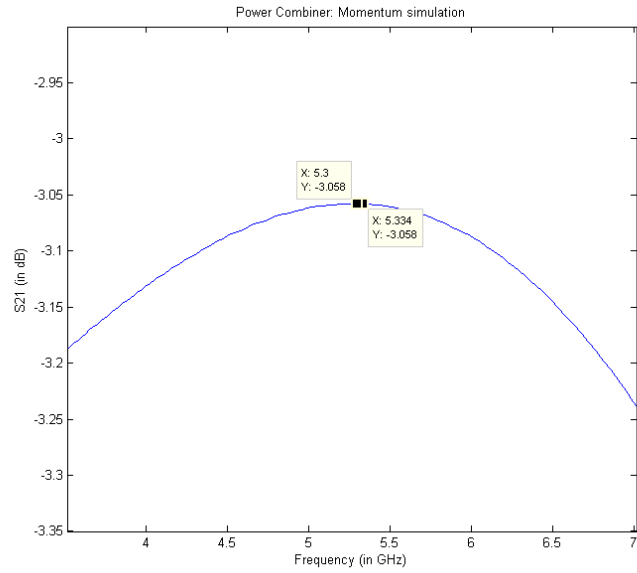


Figure 5.22: Comparison of S21 for the Wilkinson power combiner for the ERS-2 and ENVISAT centre frequencies

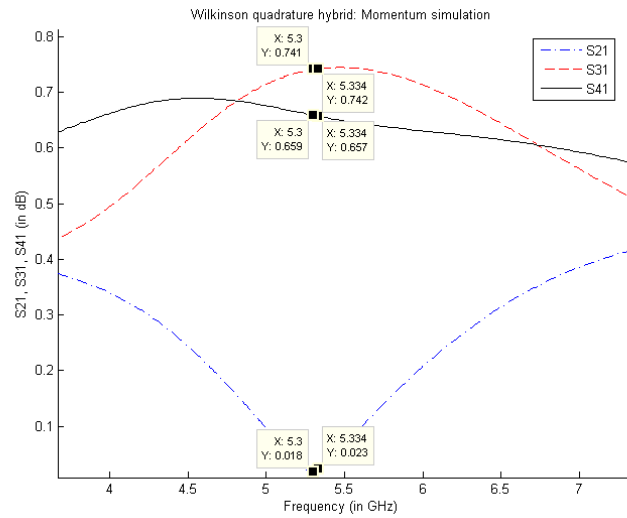


Figure 5.23: Comparison of S21, S31 and S41 for the Wilkinson quadrature hybrid for the ERS-2 and ENVISAT centre frequencies

The IQ modulator was first tested with a singletone at 10 MHz with a power of 0 dBm applied on the IF port of one of the mixers and the local oscillator signal at 5.3 GHz applied on the Wilkinson quadrature hybrid input (which eventually ends up at the LO port of that mixer). The output of the IQ modulator (which is also the output of the Wilkinson power combiner) was measured and the good behaviour of the mixer is shown in Figure 5.24: a frequency component at $(5300 + 10) \text{ MHz}$ and one at $(5300 - 10) \text{ MHz}$ both with a loss of about 10 dBm (roughly), which is still $\pm 9 \text{ dB}$ higher than the LO component. This loss is a confirmation of the predicted loss in section 3.1.5: sum of the mixer loss and power combiner loss.

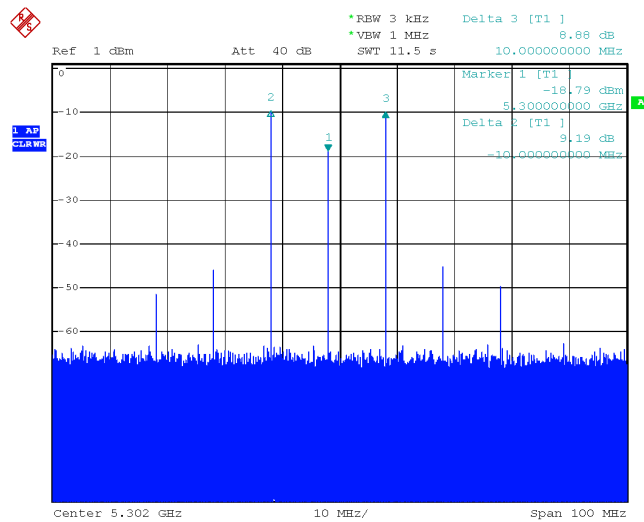


Figure 5.24: Output of the IQ modulator when applying a singletone on the IF port of one of the mixers

Finally the in-phase and quadrature chirp signals provided by the two DDS's were applied to the IF port of each mixer and the local oscillator at 5.3 GHz applied on the Wilkinson quadrature hybrid input. The output of the IQ modulator was measured and the good behaviour is shown in Figure 5.25: a single side band, here the lower side band, around LO frequency (5.3 GHz).

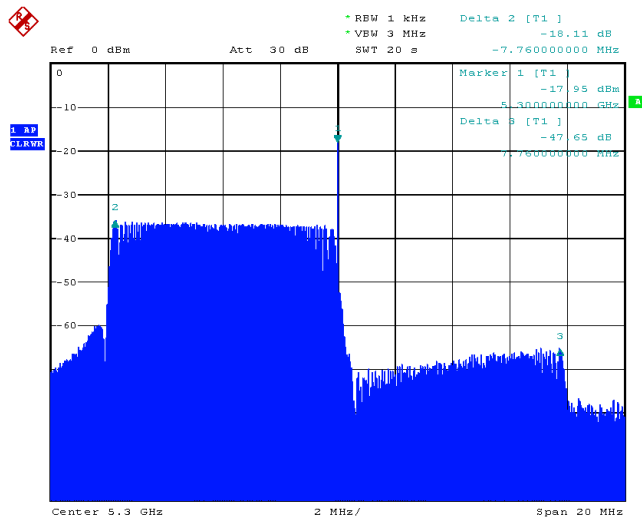


Figure 5.25: Output of the IQ modulator when applying an in-phase and quadrature chirp signal on the IF input ports

The linear sweep of the DDS's is not continuously going up to 8 MHz and down to DC: it stays for a relatively short period of time at DC. When the signal is upconverted during this time, it gives the high frequency component at 5.3 GHz with a power level higher than that of the side band.

In Figure 5.26 the IQ modulator in its metallic box is shown.

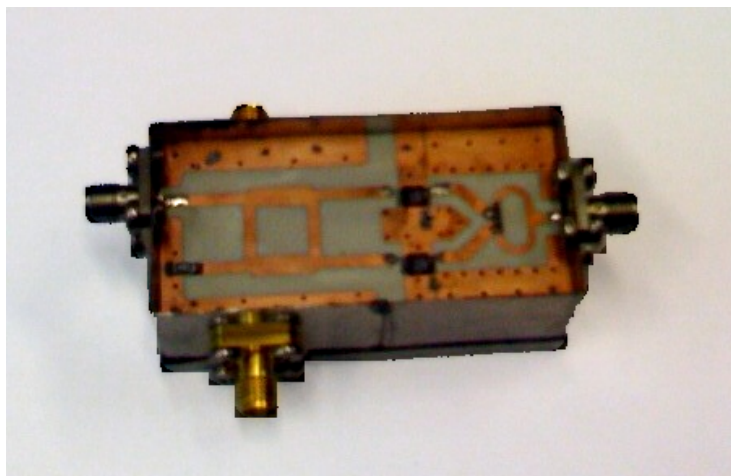


Figure 5.26: Picture of the IQ modulator in its metallic box

5.5 Band-Pass Filter

This filter has to filter out the harmonics of the local oscillator (LO), i.e. at multiples of f_{LO} or $n \times 5.300$ GHz, unwanted intermodulation products at $n \times f_{LO} \pm f_{IF}$ and harmonics of the latter ones for $n \in \mathbb{N}_0 \setminus 1$. This means that at 10.6 GHz the signal should be greatly (roughly tens of dB's) reduced. And around 5.300 GHz at least a pass-band of ± 100 MHz should be provided as a tolerance for the difficulty of achieving the same results with manufactured high-frequent filters as within the simulations.

With the Design Assistant of ADS a coupled-line maximally flat band-pass filter was designed.

A first attempt with lower stop frequency $f_{s1} = 4.6$ GHz, lower pass frequency $f_{p1} = 5.25$ GHz, upper pass frequency $f_{p2} = 5.35$ GHz, upper stop frequency $f_{s2} = 6.0$ GHz and selectivity $k = \frac{f_{p2} - f_{p1}}{f_{s2} - f_{s1}} = 0.07$ provides 8 dB insertion loss at 5.300 GHz simulated with Momentum (see Figure 5.27), this is intolerable.

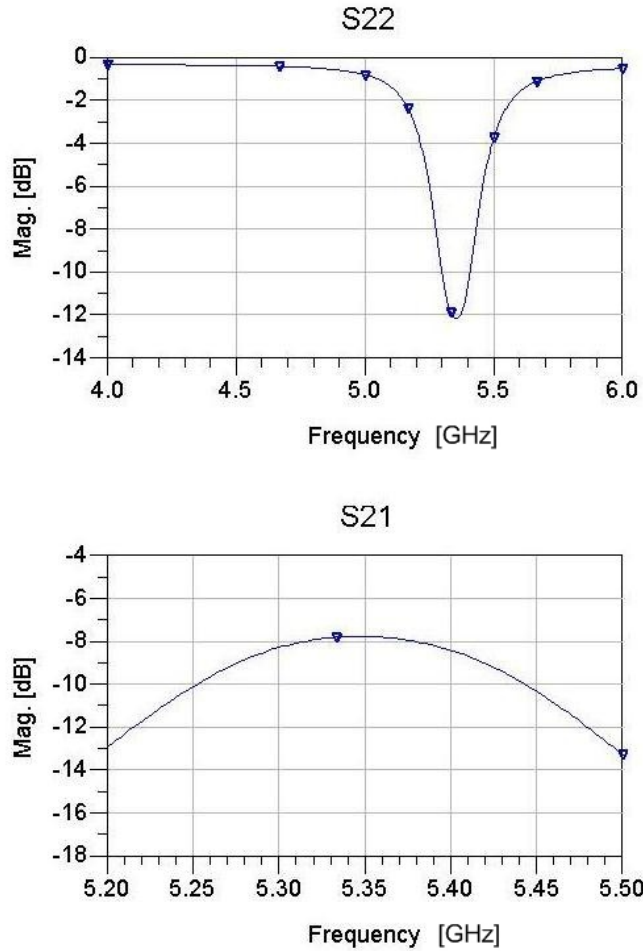


Figure 5.27: Band-pass filter with roughly 8 dB insertion loss at 5.333 GHz

A second attempt with higher selectivity k , more components in the lumped design and more coupled lines with $f_{s1} = 4.8$ GHz, $f_{p1} = 5.15$ GHz, $f_{p2} = 5.55$ GHz, $f_{s2} = 5.9$ GHz and selectivity $k = 0.36$ give 0.966 dB loss at 5.333 GHz and 1.523 dB loss at 5.264 GHz simulated with Momentum (see Figure 5.28). The interpolated value at 5.300 GHz would give a loss of 1.232 dB which is acceptable. As can also be seen on Figure 5.28 the second harmonic at 10.600 GHz is very well attenuated, based on the data point at 10.770 GHz with attenuation of 34.828 dB.

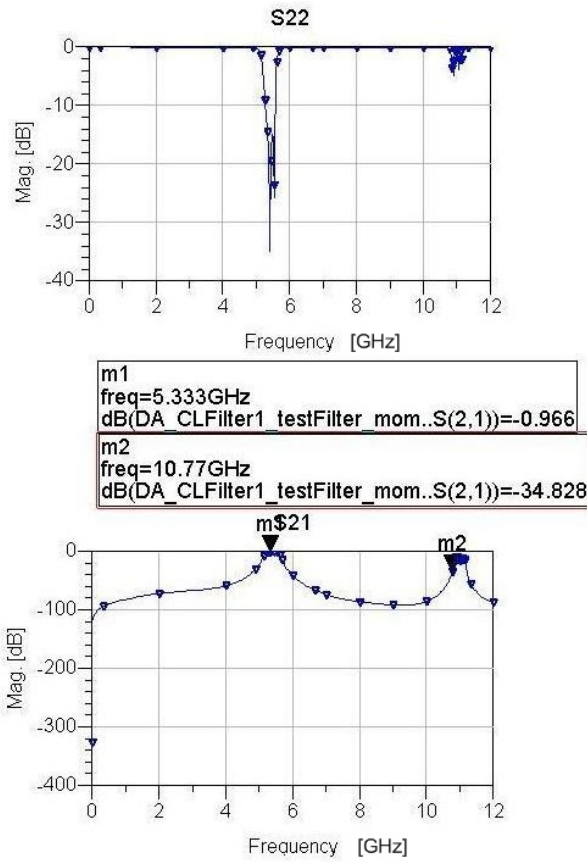


Figure 5.28: Band-pass filter with roughly 1 dB insertion loss at 5.333 GHz

The layout of this band-pass filter which was created with EAGLE is shown in Figure 5.29.

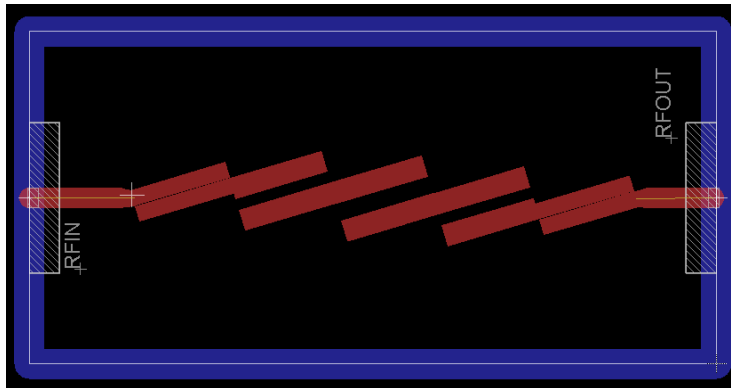


Figure 5.29: Layout of the band-pass filter, created with EAGLE

After calibration of the PNA-X Network Analyzer an S-parameter measurement was done (see Figure 5.30). At marker 4 an insertion loss of 3.350 dB is measured at 5.294 GHz, compared to the simulated insertion loss of 0.966 dB at 5.333 GHz this is a big difference but still acceptable. But the insertion loss of roughly 6 dB at 10.6 GHz is not acceptable compared to the simulated insertion loss of 34.828 dB at 10.77 GHz.

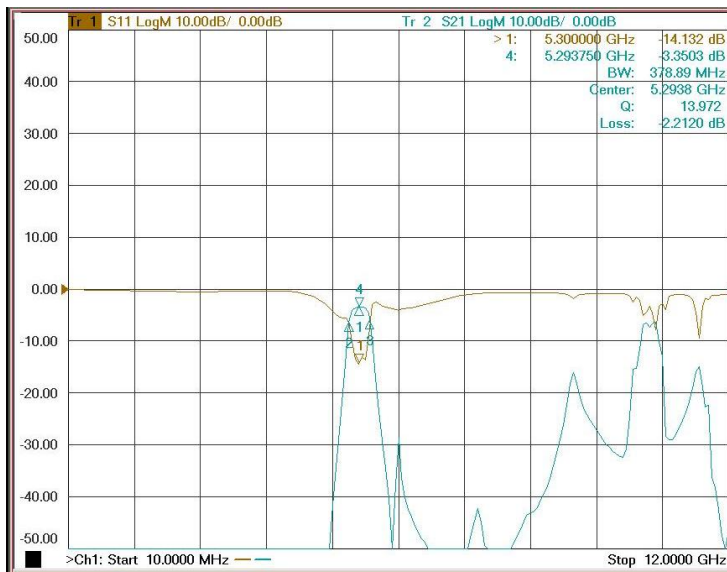


Figure 5.30: S-parameter measurement of the band-pass filter (without anti-reflection)

This can be explained by the reflections of the metallic box where the band-pass filter is put in order to remove interferences between the transmitter and

the receiver. In ADS' Momentum, a boxed transmission line model (Box & Waveguide menu) exists to simulate these side effects but it takes more CPU time. If we attenuate these reflections by putting an absorptive layer; e.g. very porous mousse, between the filter plate and the box cover, we obtain a much better result of maximum 14.479 dB attenuation in the first harmonic frequency region (see Figure 5.31).

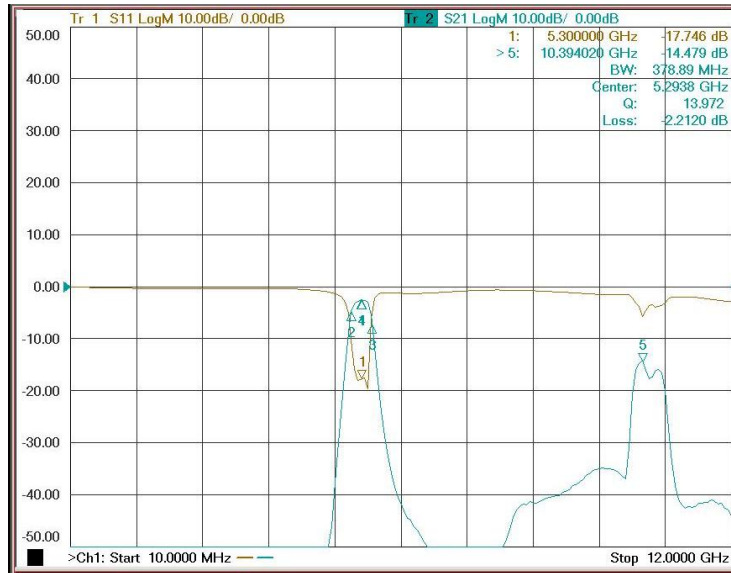


Figure 5.31: S-parameter measurement of the band-pass filter (with anti-reflection)

In Figure 5.32 the filter is shown in its metallic box, together with the mousses that were used.

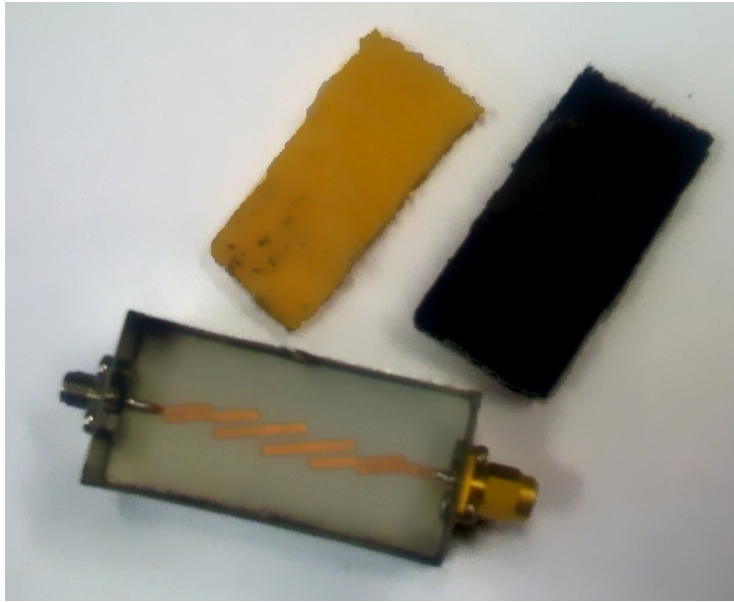


Figure 5.32: Picture of the band-pass filter in its box and the absorptive mousses

5.6 Low-Noise Amplifier and Power Amplifier

For the layouts of the low-noise amplifier and the power amplifier, following the advice of the manufacturer Hittite, it is chosen for a coplanar waveguide design with back ground plane (instead of microstrip for the IQ modulator) and a substrate height H of 0.5 mm (instead of $H = 0.8$ mm). With LineCalc a new $50\ \Omega$ width is calculated at 5.300 GHz, which gives a width of 34.706 mils or 0.882 mm (instead of 68.879 mils or 1.750 mm). Now the transition of the $50\ \Omega$ line width to the thinner pins of the amplifiers is not so abrupt anymore which results in less radiation from the RF input line to the RF output line of the amplifiers.

The layout of the low-noise amplifier is given in Figure 5.33 and the layout of the power amplifier is given in Figure 5.34.

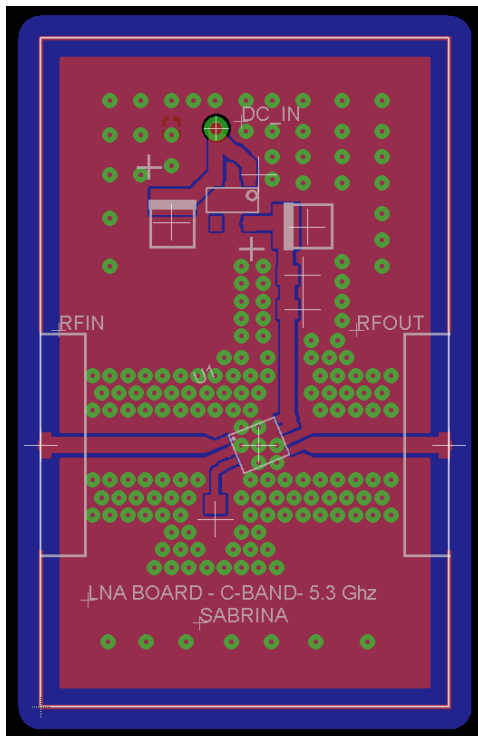


Figure 5.33: Layout of the LNA board, created with EAGLE

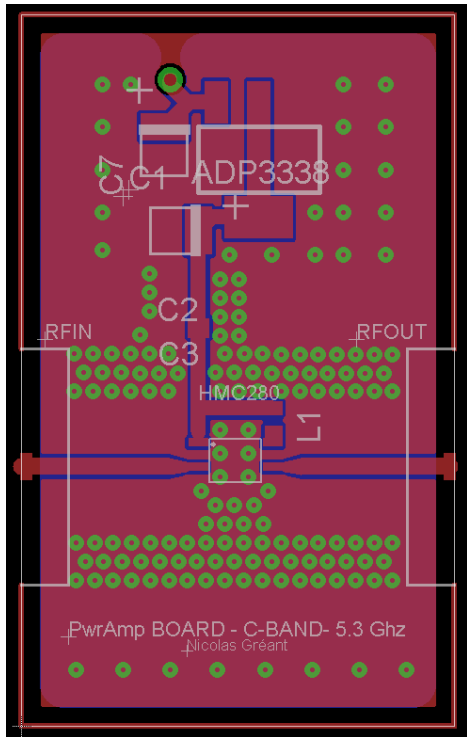


Figure 5.34: Layout of the power amplifier board, created with EAGLE

These subsystems could not be finished in time by the technicians although the layouts were handed in quite some time before the project deadline. This is a pity but not a disaster as they do not really change the frequency spectrum, except for amplifying frequency components. Moreover, on the presentation of this project they will be added to the output of the IQ modulator so that the amplified output can be shown.

Chapter 6

Conclusion

In this project most of the time was spent on the analog microwave design and layout as this is the most delicate part. These exertions resulted in an excellent behaviour of the IQ modulator, the most important design. This was the result of intensive simulation and optimization of the subsystems, in particular the Wilkinson quadrature hybrid and the Wilkinson power combiner. The band-pass filter which had to be put in between the low-noise amplifier and power amplifier proved that it filtered out the harmonics well too. Unfortunately the amplifiers could not be build in time but they are not crucial to prove that the expected chirp signal can be obtained and they still will be ready for the presentation of the project.

On the base band level, the programming of the DDS and especially the synchronization of both in-phase and quadrature outputs was a though challenge. Testing on the oscilloscope and on the spectrum analyzer after many trial-and-error finally was fruitful. The low-pass filter is a minor subsystem of the transmitter which correctly filters out the system clock of the DDS.

A direction for further work can consist of building an X-band test transmitter at 9.65 GHz for the TerraSAR-X satellite for which a receiver front-end is being built.

The overall conclusion is that this project was a great success. The researcher coped with a big challenge, systematically subdividing it in smaller problems and so clearing away solvable obstacles. In this way it literally started from nothing and ended up with the favorable working of this test transmitter, meeting all the objectives.

It will for sure be one of the required assets for further groundbreaking developments in the SAR research domain which the researcher can be proud of.

Bibliography

- [1] K.C. Gupta; Ramesh Garg & I.J. Bahl. *Microstrip Lines and Slotlines*. Artech House, Norwood, 2nd edition, 1996.
- [2] A. Broquetas. Course on RADAR. Department TSC, Universitat Politècnica de Catalunya.
- [3] CadSoft. <http://www.cadsoft.de/>.
- [4] Rogers Corporation. <http://www.rogerscorp.com/>.
- [5] ADS 2008 Documentation. <http://edocs.soco.agilent.com/display/ads2008u2/>.
- [6] Bassem R. Mahafza & Atef Z. Elsherben. *MATLAB Simulations for Radar Systems Design*. Chapman & Hall/CRC, Boca Raton, FL, 2004.
- [7] IEEE. *Standard Radar Definitions*, 1997. Std 686.
- [8] D.B. Leeson. *A Simple Model of Feedback Oscillator Noise Spectrum*. IEEE, Vol. 54 : pp. 329–330, 1966.
- [9] Stephen A. Maas. *Nonlinear Microwave Circuits*. Artech House, Norwood, 2nd edition, 1988.
- [10] Jr. Peyton Z. Peebles. *Radar Principles*. John Wiley & Sons, New York, 2nd edition, 1998.
- [11] David M. Pozar. *Microwave Engineering*. John Wiley & Sons, New York, 2nd edition, 1998.
- [12] Jesús Sanz-Marcos; Paco López-Dekker; Jordi J. Mallorquí; Albert Aguiasca & Pau Prats. *SABRINA: A SAR Bistatic Receiver for Interferometric Applications*. IEEE Geoscience And Remote Sensing Letters, Vol. 4 (No. 2): pp. 307–311, April 2007.
- [13] Paco López-Dekker; Jordi J. Mallorquí; Pau Serra-Morales & Jesús Sanz-Marcos. *Phase Synchronization and Doppler Centroid Estimation in Fixed Receiver Bistatic SAR Systems*. IEEE Transactions On Geoscience And Remote Sensing, Vol. 46 (No. 11): pp. 3459–3471, November 2008.

- [14] M. I. Skolnik. *Introduction to RADAR systems*. McGraw-Hill Book Co., Singapore, 2nd edition, 1980.
- [15] Xilinx. <http://www.xilinx.com/>.